AEGIS – Measuring the Free Fall of Antihydrogen

Alban Kellerbauer

Max Planck Institute for Nuclear Physics, Heidelberg

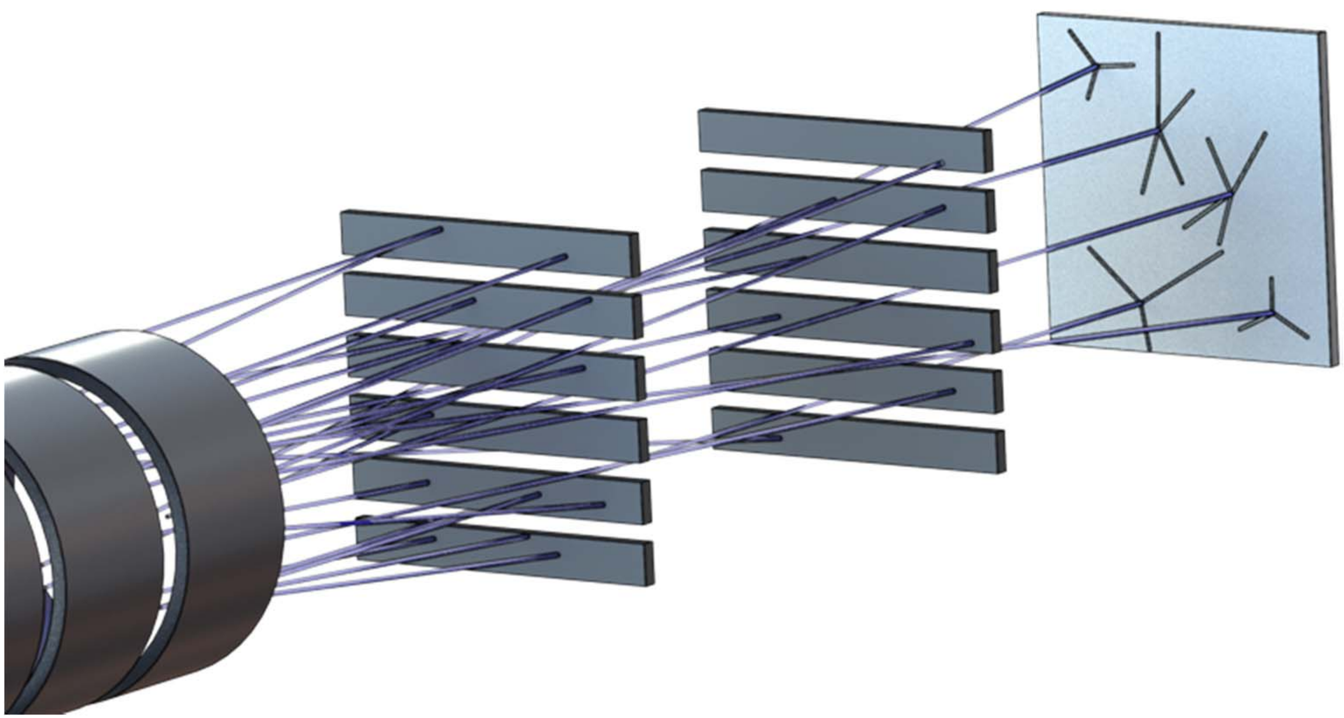

AEḡIS: Antimatter Experiment: Gravity, Interferometry, Spectroscopy

- Main goal: Measurement of *g* with 1% precision* on antihydrogen
  * (initially)
- Proposed in 1997 by Tom Phillips (Duke U)
  [T. J. Phillips, Hyp. Int. **109** (1997) 357]
- Requirements / challenges:
  - Production of a **bunched cold beam of antihydrogen** (100 mK)
  - Measurement of vertical beam deflection (10 µm drop over 1 m)

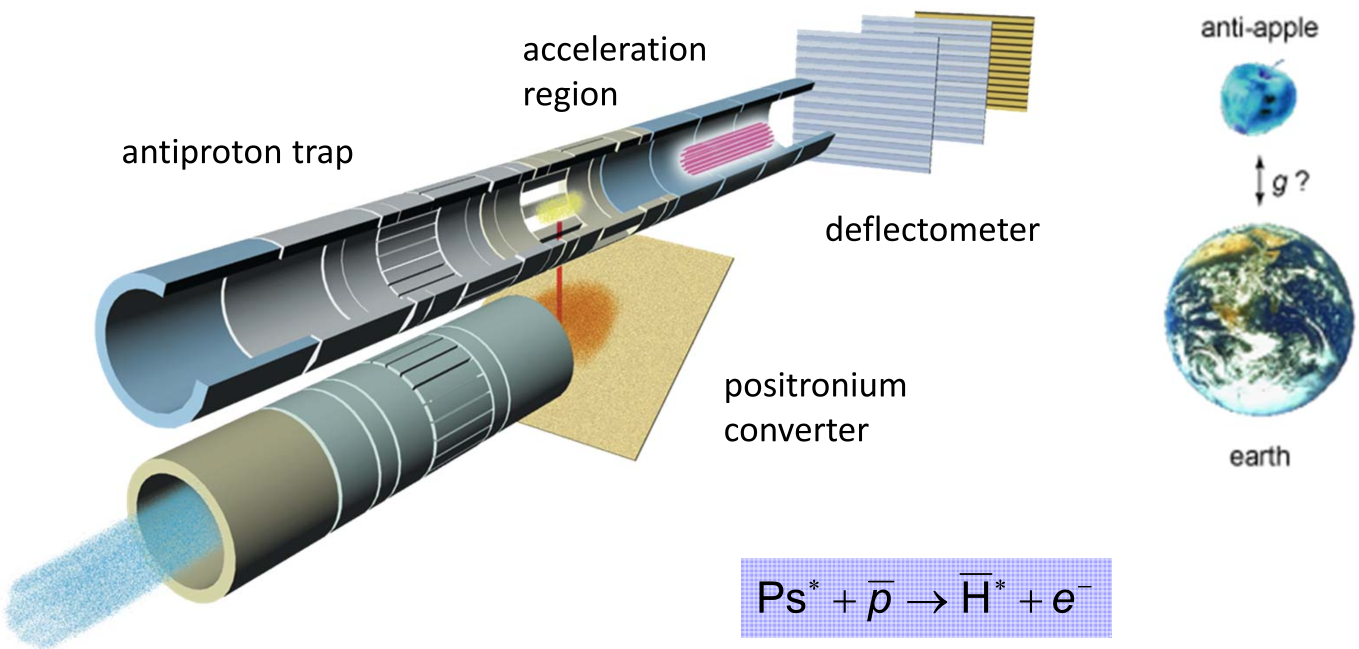

$$Ps^* + \bar{p} \rightarrow \overline{H}^* + e^-$$

Outline

- Introduction and motivation
- AEGIS principle and setup
- Current status
- Conclusions and outlook

Baryon asymmetry

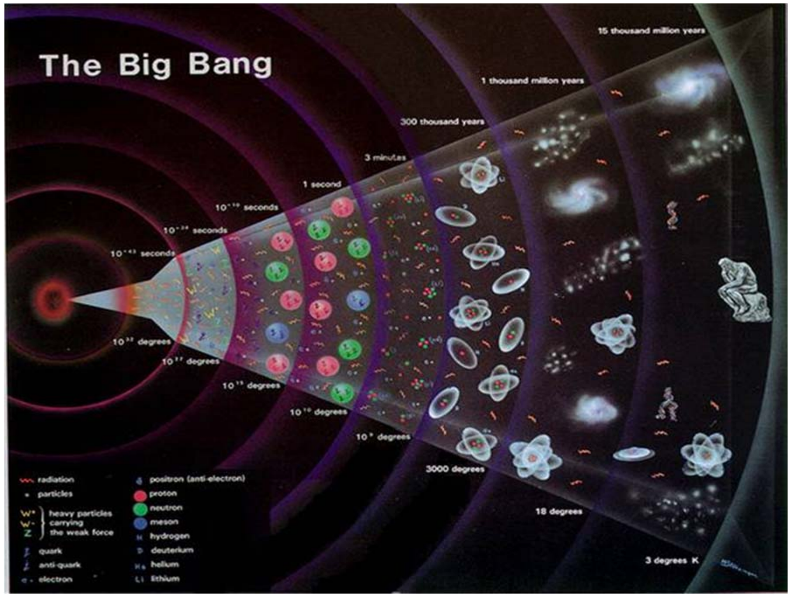

- All matter (and antimatter) was created in the big bang 13.8 billion years ago
- Most matter and antimatter annihilated to photons soon after
- But: there is some matter left!

- No evidence of (primary) antimatter anywhere in the universe today
- **1998**: AMS-01 experiment

3×10^6	He nuclei	
0	$\overline{\text{He}}$ nuclei	observed


Alpha Magnetic Spectrometer on board space shuttle Discovery

Where is the antimatter?

- Baryon asymmetry:

13.8 billion years ago:

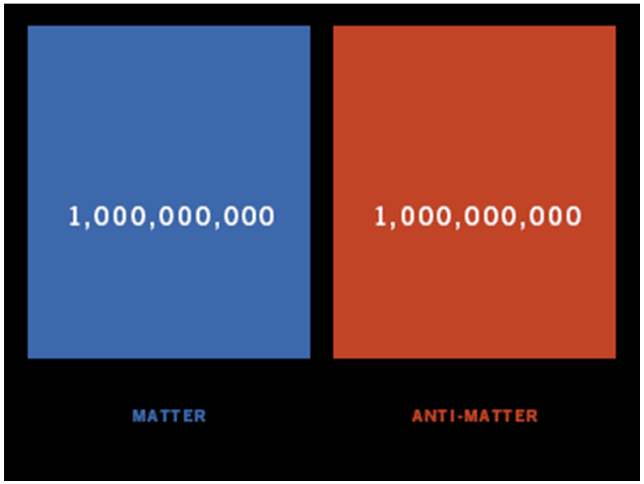

Today:

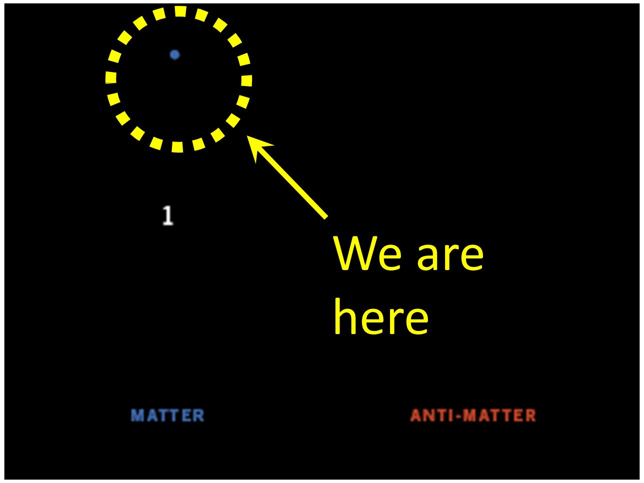

$$\frac{n(B) - n(\overline{B})}{n(\gamma)} < 10^{-9}$$

$\Rightarrow$ Tiny deviation is responsible for the existence of all baryonic matter!

- Possible explanations:

1. Difference in matter/antimatter properties (CP or CPT violation)

2. Anomalous gravitation, segregation in different parts of the universe

Precision tests with antimatter

- Test of CPT symmetry

  Baryon asymmetry

  ⇔ difference in properties ?

  C – charge conjugation

  P – inversion of spatial coordinates

  T – time reversal

  $\overline{m}_\mathrm{i} \stackrel{?}{=} m_\mathrm{i}$ $\overline{q} \stackrel{?}{=} q$ $\overline{g}_\mathrm{S} \stackrel{?}{=} g_\mathrm{S}$ etc.

- Antimatter gravity

  Test of weak equivalence principle with antimatter

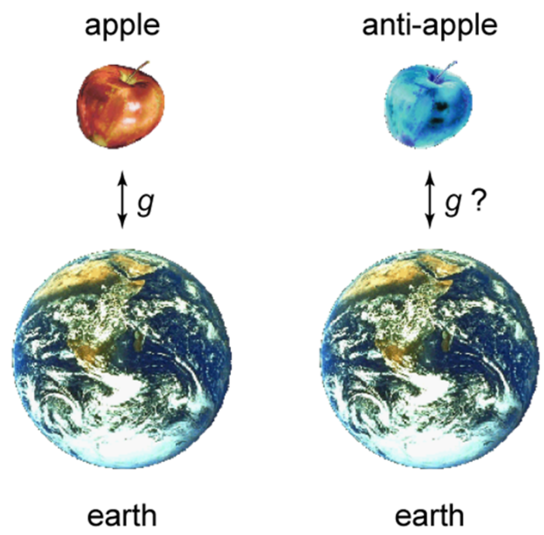

$\overline{m}_\mathrm{g} \stackrel{?}{=} \overline{m}_\mathrm{i}$

- Since 2002 copious amounts of neutral antiatoms available

  ⇒ antihydrogen is an ideal test body for these fundamental tests

  [M. Amoretti *et al.*, Nature **419** (2002) 456; G. Gabrielse *et al.*, Phys. Rev. Lett. **89** (2002) 213401]

Antimatter gravity

- Weak equivalence principle (WEP):

  "The trajectory of a falling test particle is independent of its composition."

- WEP extremely well tested with matter, but never with antimatter (electric charge of subatomic particles)

$$\overline{m}_g \overset{?}{=} \overline{m}_i$$

- Gravity is the only force not described by a quantum field theory
- QFT formulations of gravity open the way for
  - Non-Newtonian gravity
  - WEP violation
  - Fifth forces etc.

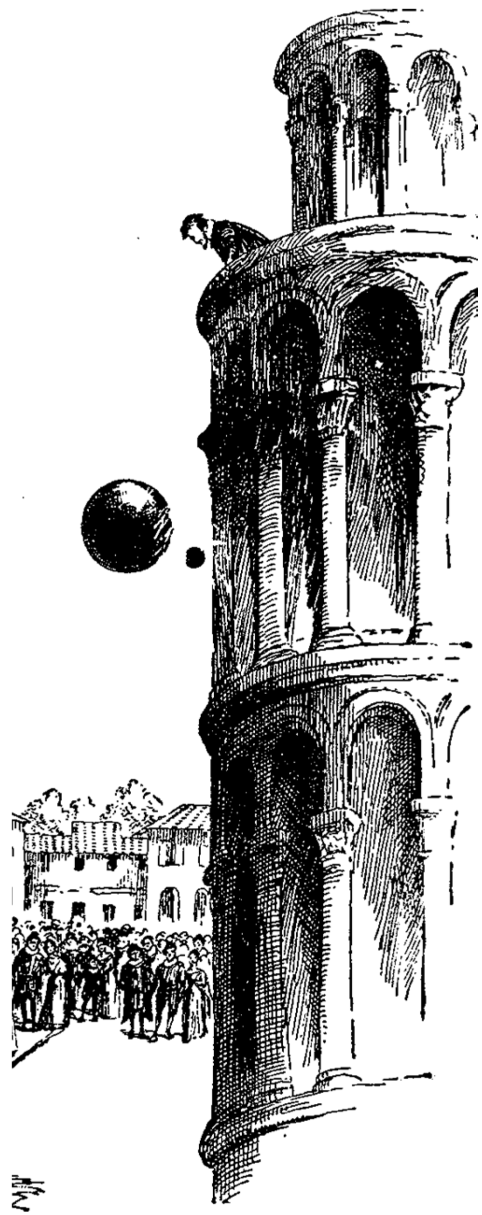

Quantum gravity

- Quantum gravity could accommodate non-Newtonian components (scalar, vector), coupling to various charges…
- Hypothetical exchange particles:

• Tensor graviton	(Spin 2, "Newtonian")	always attractive
• Vector graviton	(Spin 1)	repulsive between like charges
• Scalar graviton	(Spin 0)	always attractive

- Quantum gravity potential (static limit):

$$V = -\frac{Gm_1m_2}{r}\left(1 \pm \alpha_v e^{r/\lambda_v} + \alpha_s e^{r/\lambda_s}\right)$$

where α_v, λ_v – vector c.c./range
α_s, λ_s – scalar c.c./range

- Non-Newtonian terms could (almost) cancel out if $\alpha_v \approx \alpha_s$ and $\lambda_v \approx \lambda_s$, but produce a striking effect on antimatter

The Morrison argument

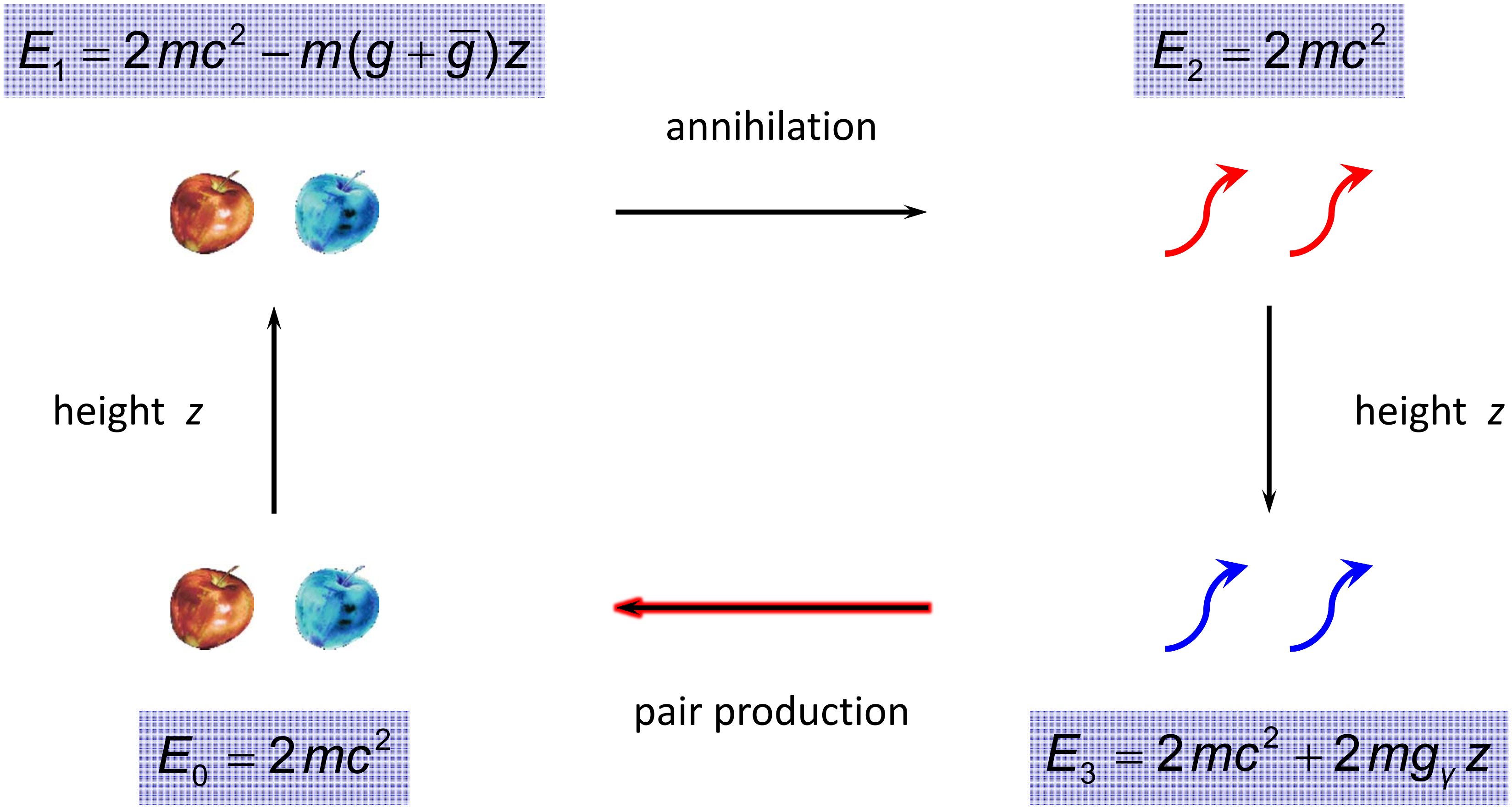

- Energy conservation violated if $\bar{g} = -g$
- Valid argument against anti-*tensor* gravity
- Irrelevant for other scenarios (scalar/vector, other couplings)

[P. Morrison, Am. J. Phys. **26** (1958) 358;
M. M. Nieto & T. Goldman, Phys. Rep. **205** (1991) 221]

Indirect experimental limits on antigravity

A. "Newtonian experiments" (force / acceleration / deflection)

- Eötvös-type experiments, "Fifth force" searches
- Fraction of nuclear mass due to virtual antiquarks

→ Coupling of gravity to virtual particles not understood; antimatter content fractions between different nuclides might not differ

B. "Einsteinian experiments" (red shift / rescaling of observed time)

- $p/\bar{p}$ cyclotron frequency, K^0–$\bar{K}^0$ non-regeneration (beyond CP violation)
- Despite CPT invariance, observed frequencies influenced by spacetime metric: $\alpha_g < 5\times10^{-4}$
- K^0–$\bar{K}^0$ oscillation rate dependent on gravitational potential: $\alpha_g < 2\times10^{-9}$

→ Depends on CPT invariance, absolute gravitational potential, choice of potential

C. Astronomical (anti-)neutrino observations

- Contribution to flavor oscillations due to gravitational potential

  Solar neutrinos: $\alpha_g < 0.2$ or 2×10^{-4}, depending on potential (Earth, galactic supercluster)
- Supernova SN1987A $\nu/\bar{\nu}$ arrival time: $\alpha_g < 0.5\%$ (galactic supercluster)

→ Restricted to neutrino sector; depends on absolute gravitational potential

[T. Ericson & A. Richter, Europhys. Lett. **11** (1990) 295; E. Adelberger *et al.*, Phys. Rev. Lett. **66** (1990) 850; M. M. Nieto & T. Goldman, Phys. Rep. **205** (1991) 221; S. Bellucci & V. Faraoni, Phys. Rev. D **49** (1994) 2992; M. Fischler *et al.*, Fermilab report FN-0822-CD-T (2008)]

Did I say "never been measured"?

- ALPHA: 2013 reanalysis of 2010/2011 data
- Release of $\bar{H}$ from magnetic trap at 0.5 K (trap shutoff time constant $\tau \approx 9.5$ ms)
- 434 annihilation events observed

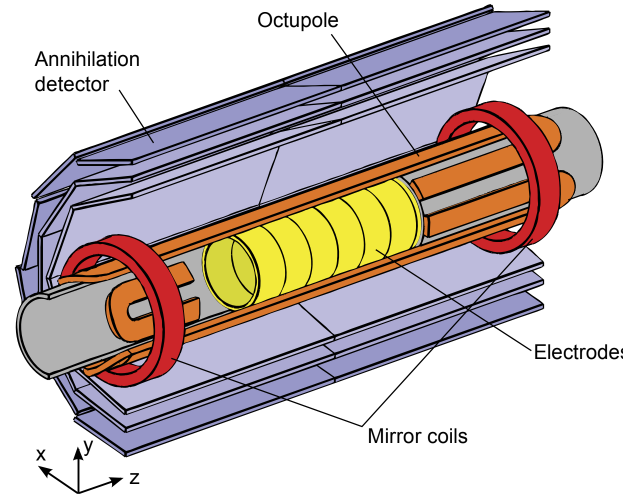

- Vertical position of annihilations:

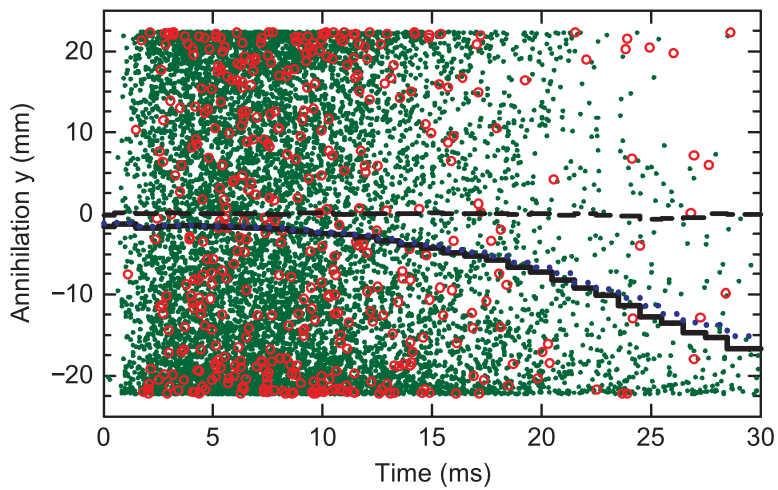

  - red circles: data
  - green dots: simulation for $\bar{g}/g = 100$

[C. Amole *et al.*, Nature Comm. **4** (2013) 1785]

- Result:

$$\bar{g} = (-65..+110)\ g$$

(95% confidence level)

- Compare with "worst case" expectation:

$$\bar{g} = (-1..+2)\ g$$

Outline

- Introduction and motivation
- AEGIS principle and setup
- Current status
- Conclusions and outlook

Antiproton Decelerator at CERN

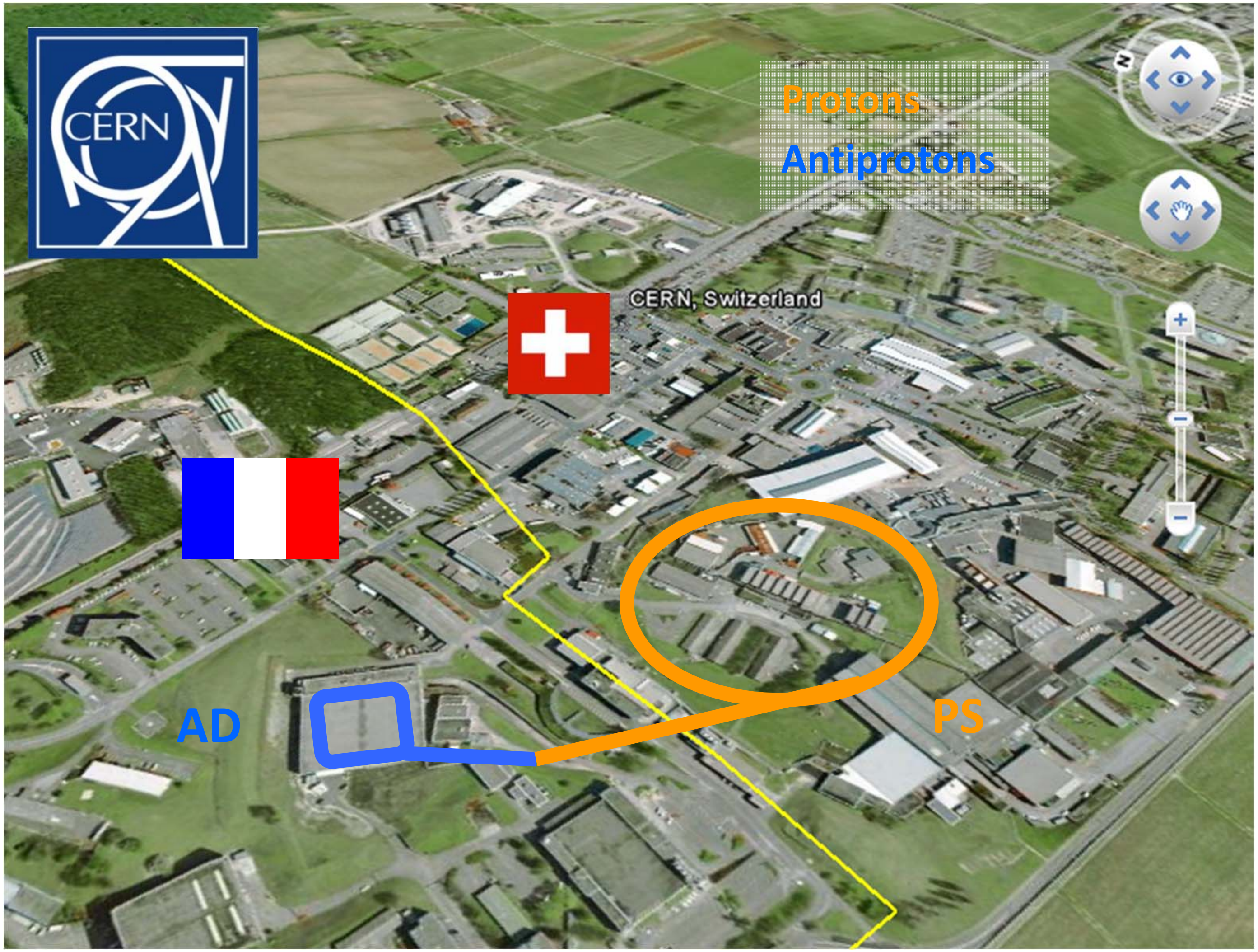

- 10^7 $\bar{p}$ produced every ≈ 90 s
- Deceleration p = 3.5 GeV/c $\rightarrow$ 100 MeV/c
- Fast extraction (200-ns bunches)

AD experiments

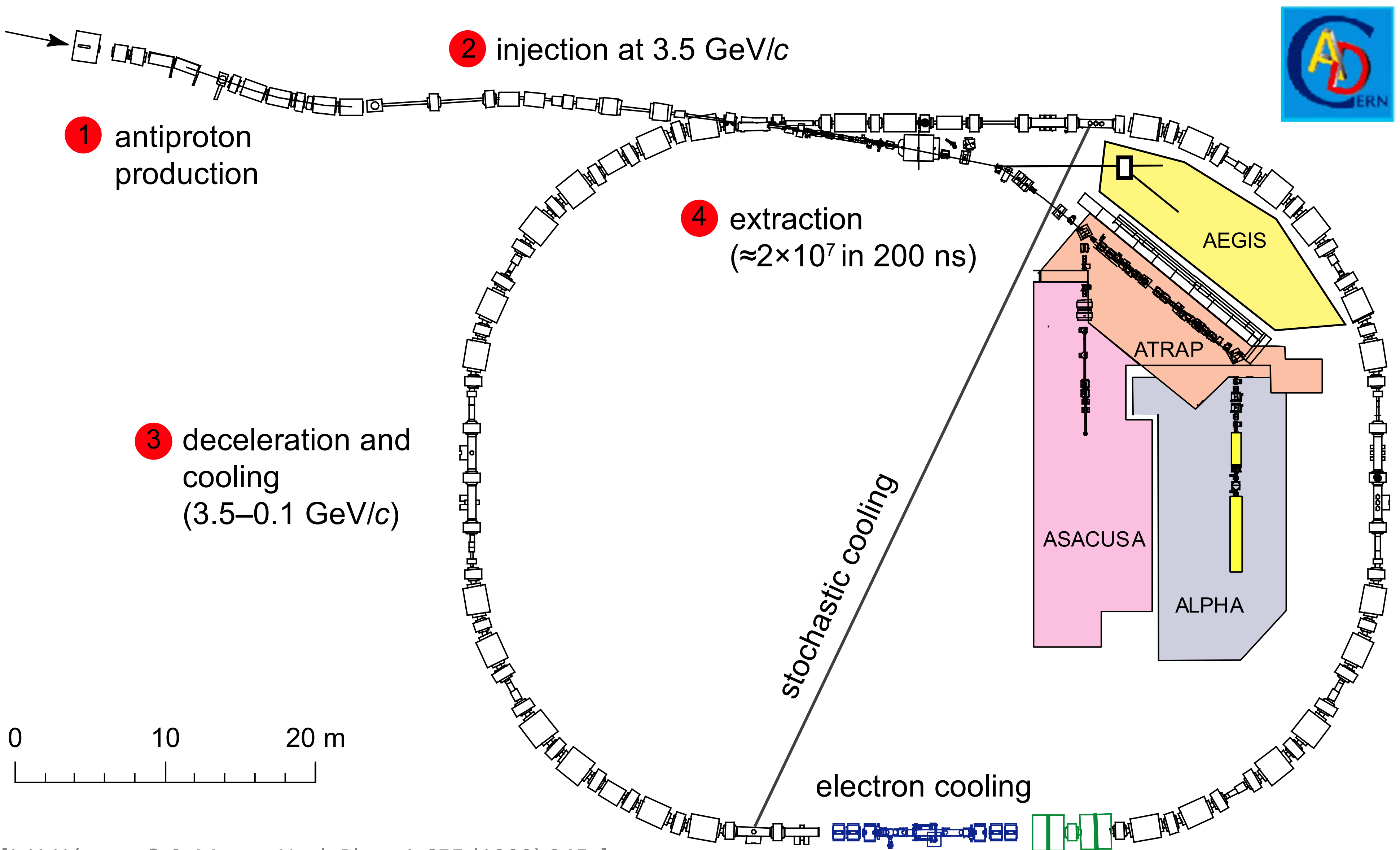

[J. Y. Hémery & S. Maury, Nucl. Phys. A **655** (1999) 345c]

Antiproton Decelerator hall

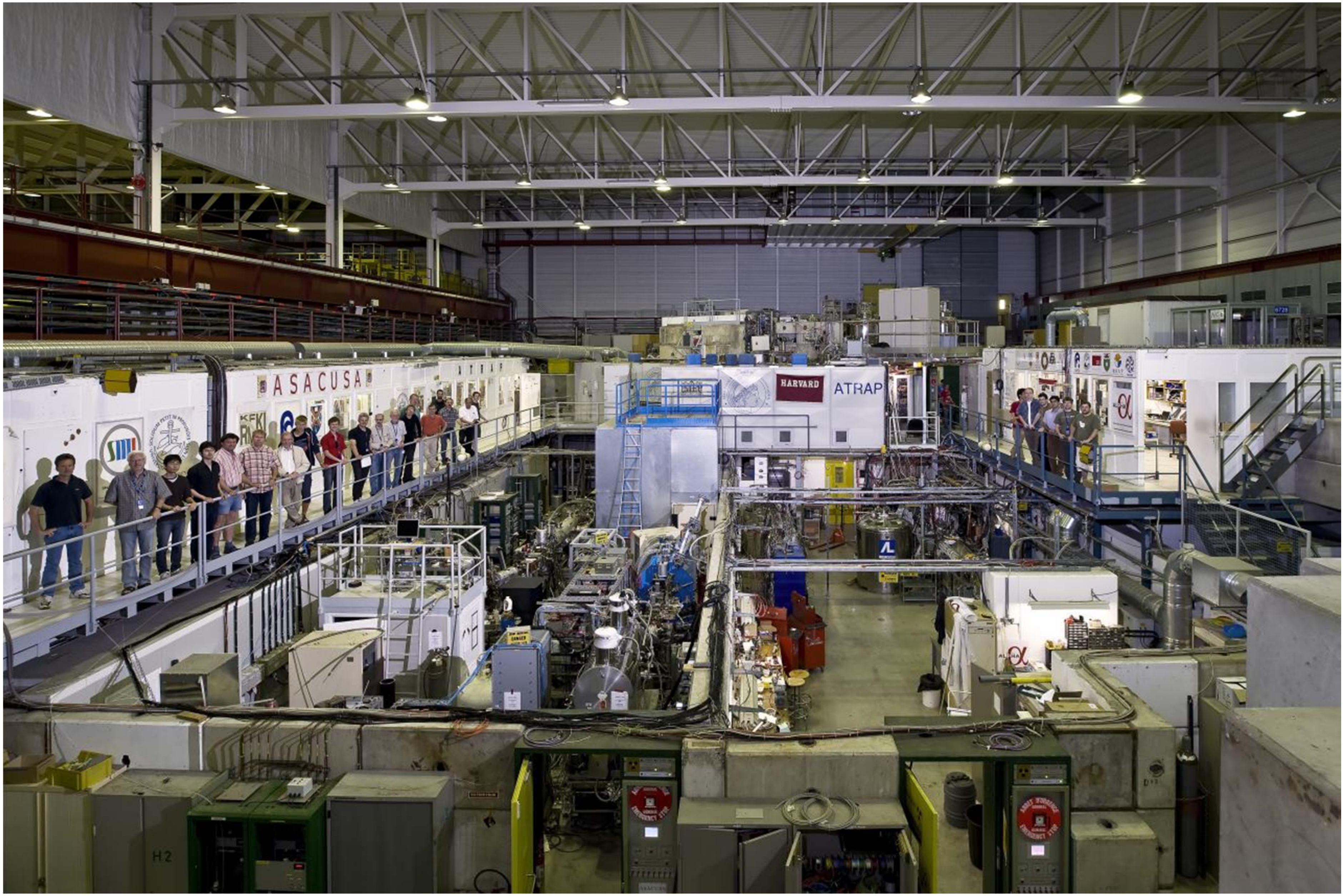

Experimental sequence

- Principle sketch (not to scale):

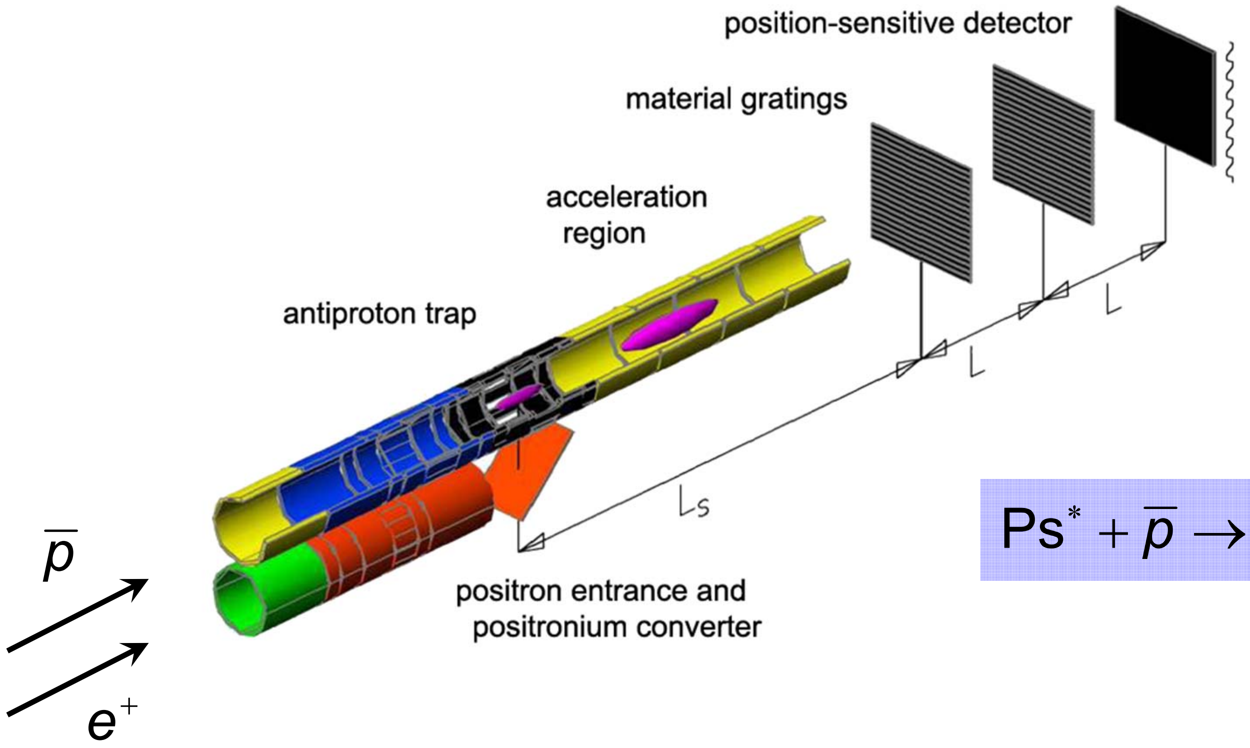

$$\mathrm{Ps}^* + \bar{p} \rightarrow \bar{\mathrm{H}}^* + e^-$$

1) Antiproton capture & cooling
2) Positron production
3) Positronium conversion
4) Positronium excitation
5) Antihydrogen recombination
6) Antihydrogen beam formation
7) Gravity measurement
8) Data analysis

AEGIS overview sketch

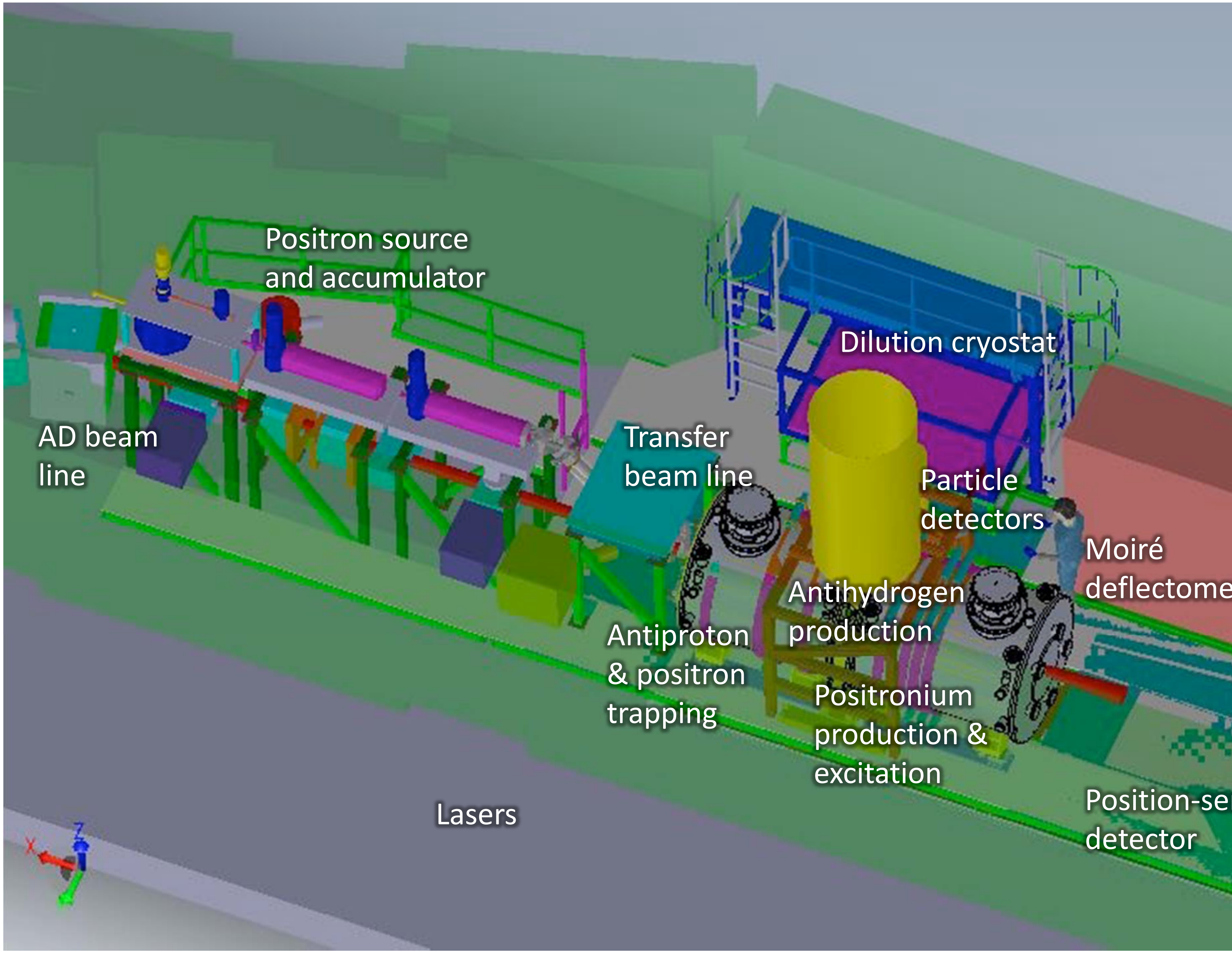

1) Antiproton capture and cooling

- Energy reduced by 50-µm Al degrader foil
- Trapping sequence:
  1. Trap is prepared with plasma of 10^8 cold electrons
  2. Small fraction of antiprotons with $E < 5$ keV is reflected
  3. Axial potential on entrance side is raised to trap $\bar{p}$
  4. Antiprotons are sympathetically cooled by electrons
- Trap cooled to 100 mK by a dilution refrigerator

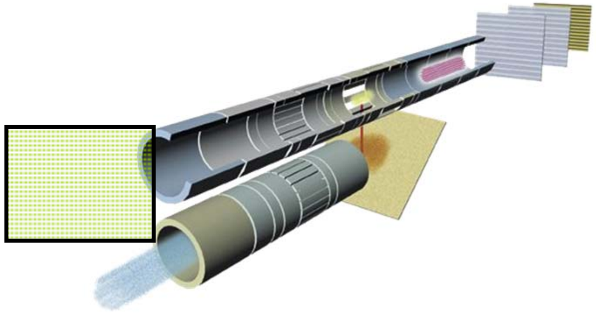

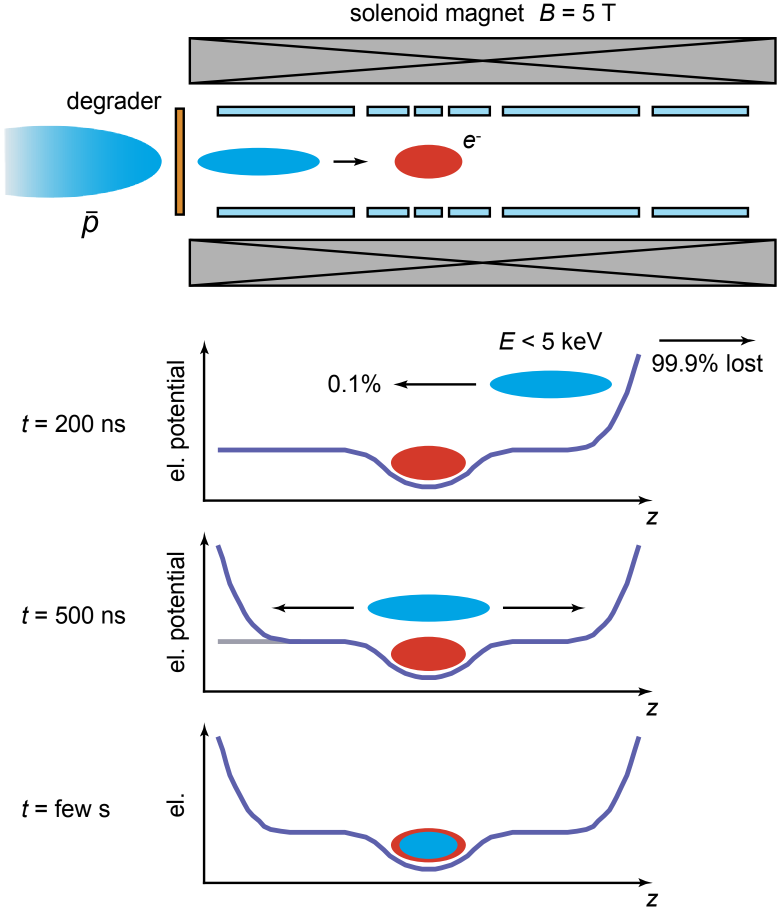

> 10^4 antiprotons @ 100 mK

2) Positron production & accumulation

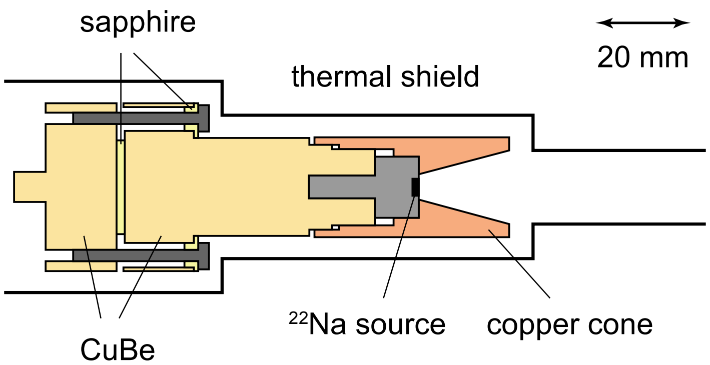

- Production from β^+ emitter:

$$^{22}\mathrm{Na} \rightarrow {}^{22}\mathrm{Ne} + e^+ + \nu_e$$

- Moderation to 50 eV in solid neon

- Trapping & cooling sequence:
  - Confinement in 0.14-T trap
  - Deceleration in N buffer gas
  - Accumulation in axial electric-field minimum

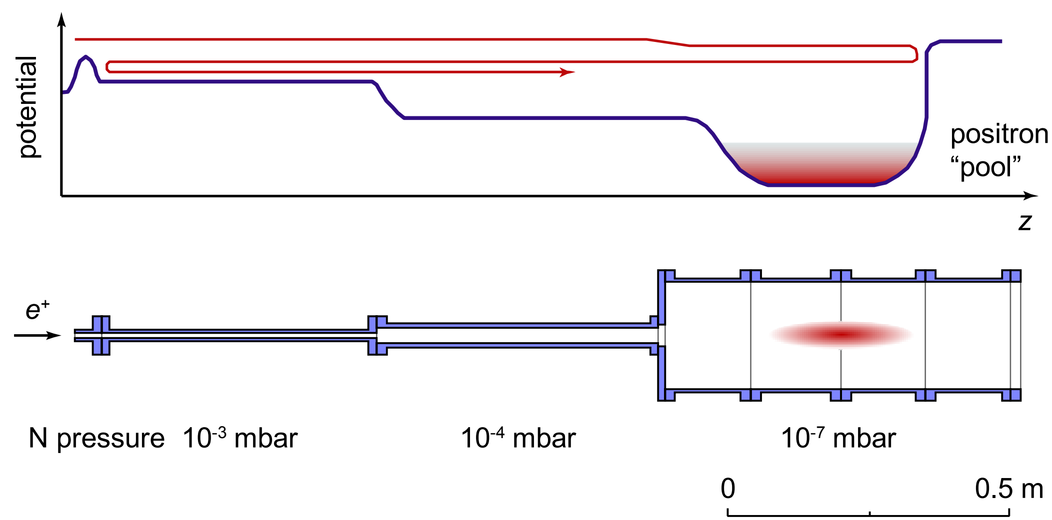

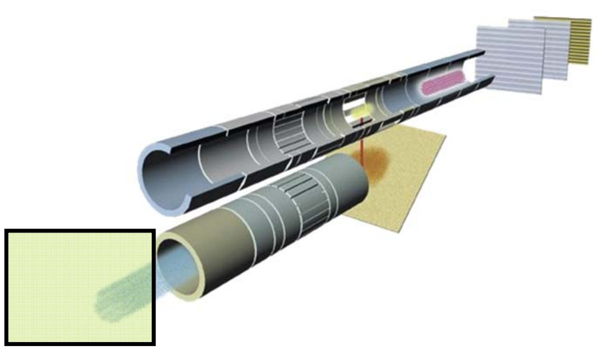

≈ 10^8 positrons every 200 s

[M. Amoretti *et al.*, Nucl. Instrum. Methods A **518** (2004) 679]

2) Positron production & accumulation

- Positron displacement by diocotron excitation:

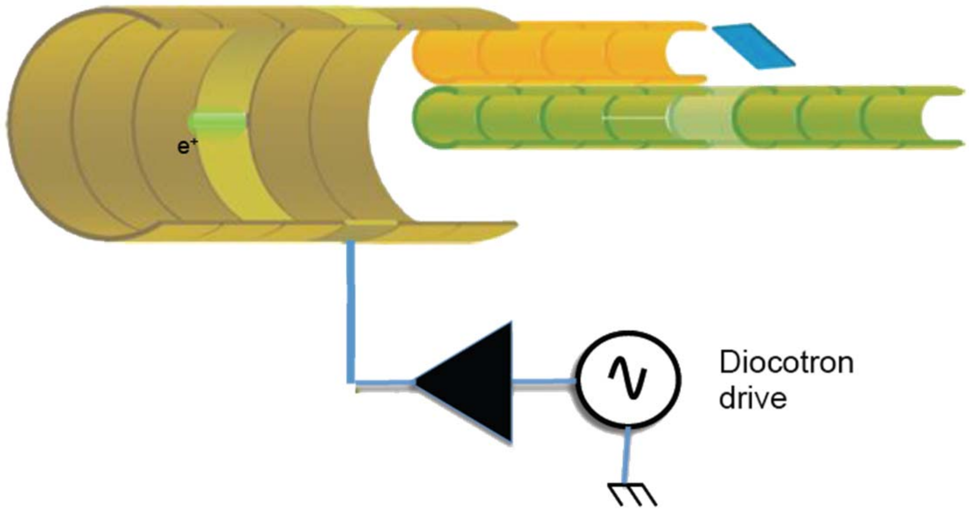

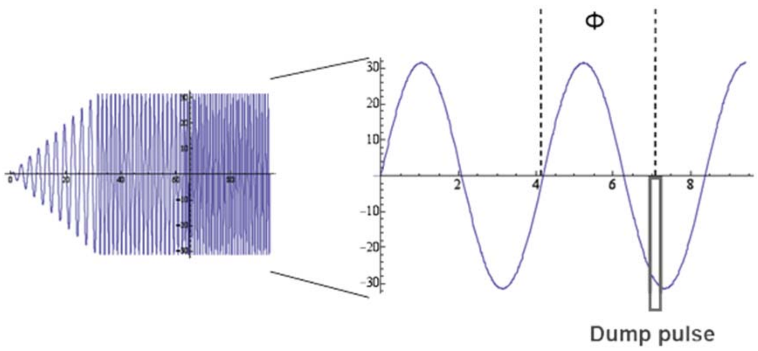

Diocotron amplitude and frequency initially increase, then stay constant at ≈ 2 V, ≈ 10 kHz

  - Plasma is brought into autoresonance with driving diocotron signal
  - Plasma moves along circular path around trap axis
  - Excitation amplitude and extraction pulse phase determine radial distance and angle

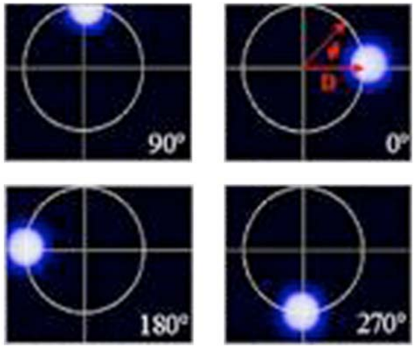

3) Positronium production

- Ps formation in nanoporous insulators:
  - Implanted positrons scatter off atoms and electrons, slow to eV in few ns
  - Positronium forms by capture of bound electrons or free electron from collisions
  - Reduced dielectric strength in defects $\Rightarrow$ accumulation of positronium in voids
  - If pores are fully interconnected, (almost) all ortho-Ps diffuses out of the film
- ortho-Ps yield and velocity distribution depend on
  - Converter material
  - Implantation depth (energy)
  - Target temperature
  - $\rightarrow$ up to 30% at 50 K

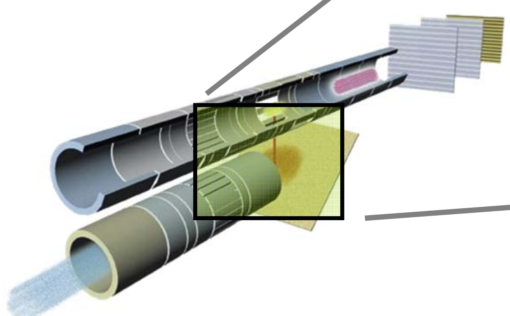

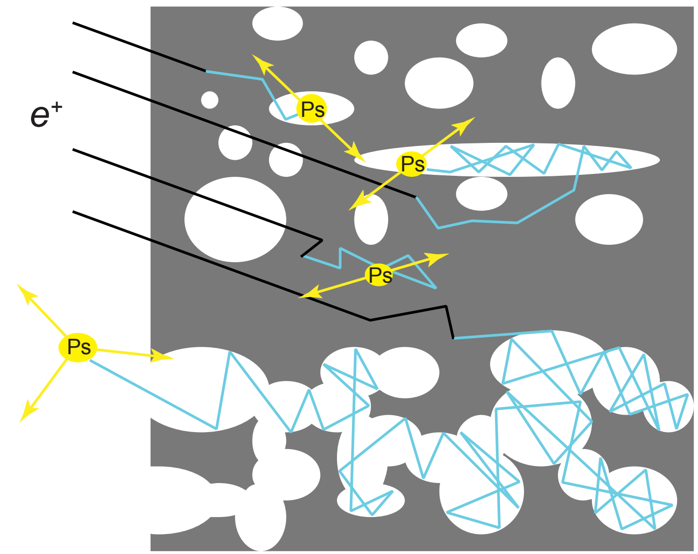

[D. W. Gidley *et al.*, Annu. Rev. Mater. Res. **36** (2006) 49]

High-efficiency positronium converter

4) Positronium excitation

- Cross-section of Ps charge exchange reaction is enhanced for large *n*: $\sigma \approx a_0 n^4$

- Two-step excitation $n = 3 \rightarrow n = 35$

  Excitation efficiency ≈ 30%

- Requirements
  - Bandwidth matched to broadened Rydberg levels
  - Sufficient power to excite Ps cloud within few ns
  - Beam tailored to geometry of expanding cloud

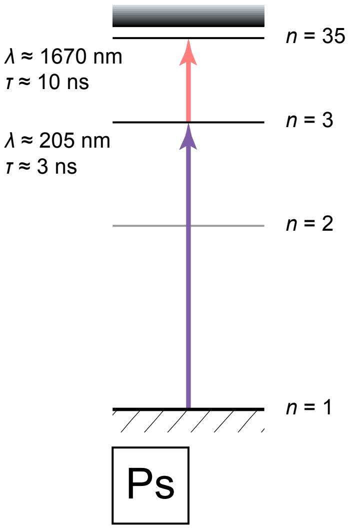

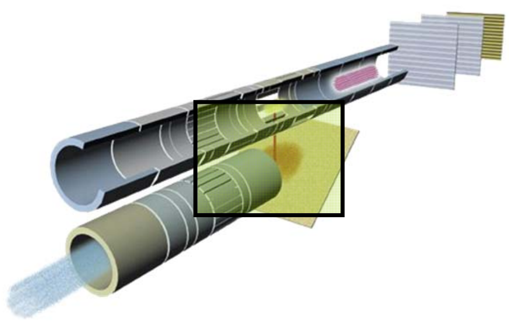

5) Antihydrogen recombination

- Charge exchange reaction:

$$\mathrm{Ps}^* + \bar{p} \rightarrow \bar{\mathrm{H}}^* + e^-$$

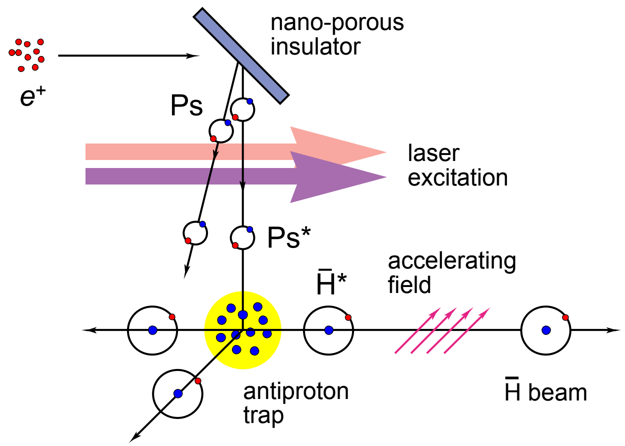

- Principle demonstrated by ATRAP
Cs* → Ps* → H̄*

[C. H. Storry *et al.*, Phys. Rev. Lett. **93** (2004) 263401]

- Advantages:
  - Large cross-section:

$$\sigma \approx a_0 n^4$$

  - Narrow and well-defined H̄ *n*-state distribution

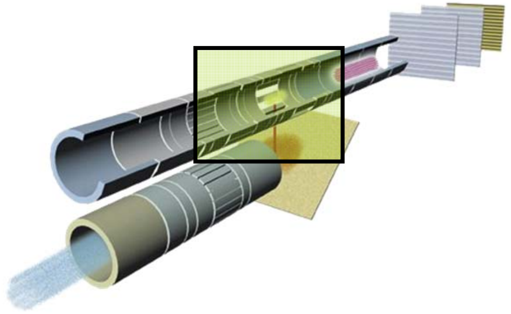

  - Antiproton temperature essentially determines antihydrogen temperature:

At $T(\bar{p})$ = 100 mK, n_{Ps} = 35
⇒ $v(\bar{\mathrm{H}}) \approx$ 45 m/s
$T(\bar{\mathrm{H}}) \approx$ 120 mK

⇒ cold / ultracold H̄

6) Antihydrogen beam formation

- Electric field gradients exert force on electric dipole moments of neutral atoms:

$$U = \frac{2}{3} e a_0 \boxed{n(n-1)} F$$

$$\mathbf{F} = -\frac{2}{3} e a_0 \boxed{n(n-1)} \nabla F$$

(max. induced dipole)

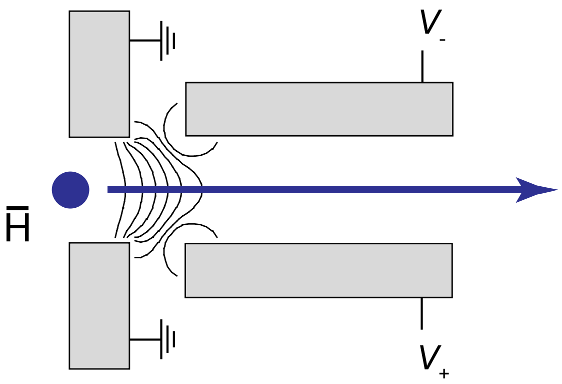

$\Rightarrow$ Rydberg atoms are very sensitive to inhomogeneous electric fields

- Stark deceleration of hydrogen demonstrated (ETH group):

[E. Vliegen & F. Merkt, J. Phys. B **39** (2006) L241]

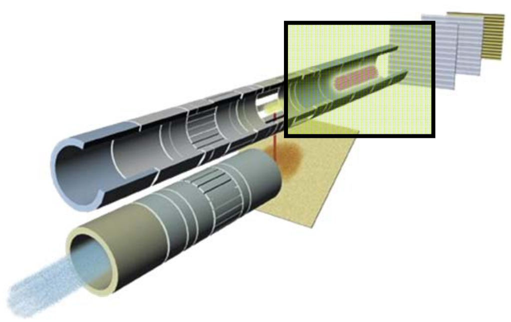

– n = 22,23,24
– Accelerations of up to 2×10^8 m/s^2 achieved
– Hydrogen beam at 700 m/s can be stopped in 5 µs over only 1.8 mm

7) Gravity measurement

- Forces can be measured with a series of slits
  - Formation of an interference or shadow pattern with two slits
  - Measurement of the vertical deflection δx with a third (analysis) slit

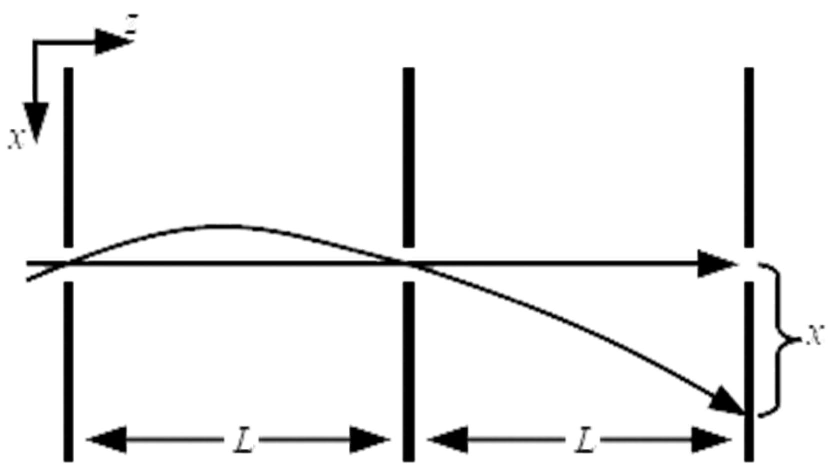

- Many slits: interferometer/deflectometer
  - Vertical deflection due to gravity:

    $\delta x \approx -10\ \mu m$

  - Vertical beam extent:

    $\Delta x \approx 5.8\ cm$

(antihydrogen beam at 100 mK, accelerated to 500 m s^{-1}, $L \approx 0.5$ m)

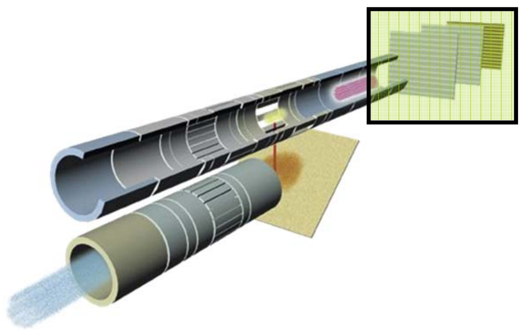

7) Gravity measurement

- Moiré deflectometer:

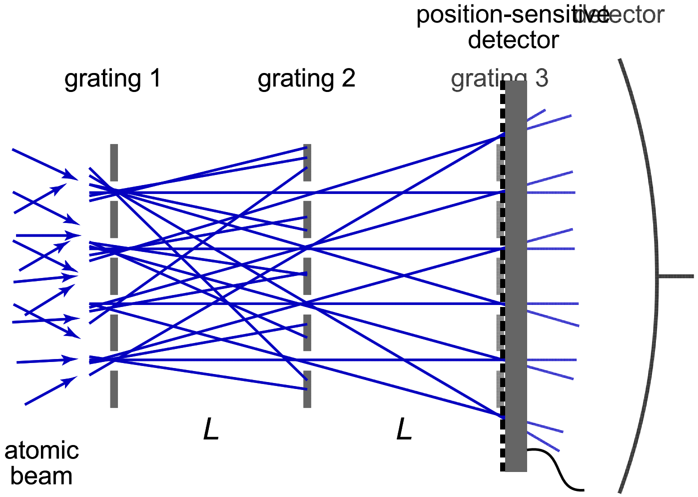

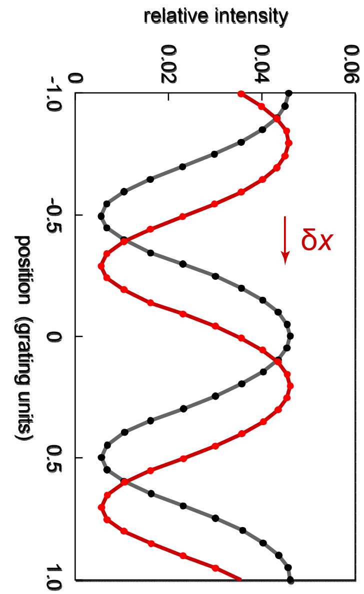

Interference pattern "falls" by

$$\delta x = -g\left(\frac{L}{v}\right)^2$$

- – Classical counterpart of Mach-Zehnder interferometer
- – Two gratings create shadow pattern on third grating
- – "Self-focusing" effect
- – Successfully used for gravity measurement on Ar atoms, $\sigma(g)/g = 2\times10^{-4}$

[M. K. Oberthaler *et al.*, Phys. Rev. A **54** (1996) 3165]

From Zehnder to moiré

- Matter-wave interferometer:

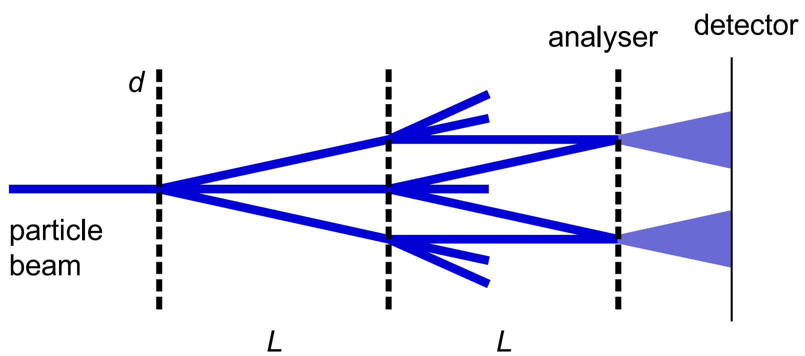

L – distance between gratings
T – TOF between gratings
d – grating period

[L. Zehnder, Z. Instrumentenkunde **11** (1891) 275;
L. Mach, Z. Instrumentenkunde **12** (1892) 89]

- Requirement on angular beam divergence:

$\delta\varphi_{\text{beam}} < \varphi_{\text{diffr}}$ $= \lambda_{\text{dB}} / d$ $\Rightarrow$ requires $T < 1$ mK (antihydrogen beam at 500 m s^{-1}, d = 100 nm)

- Solution: increase grating period

$d < \sqrt{\lambda_{\text{dB}} L}$ ⟶ $d = \sqrt{\lambda_{\text{dB}} L}$ ⟶ $d > \sqrt{\lambda_{\text{dB}} L}$

Mach-Zehnder interferometer | Talbot-Lau interferometer | moiré deflectometer

8) Data analysis

- Detection of vertical annihilation position as a function of TOF / velocity:

(Monte Carlo simulation)

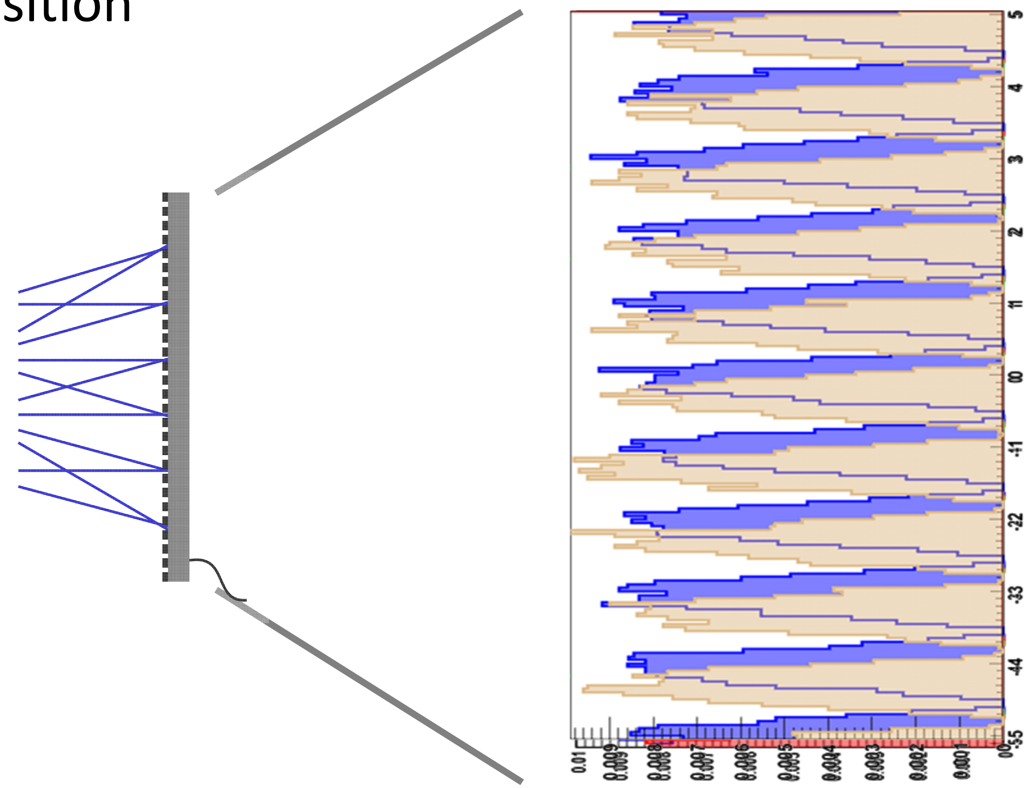

- Summing up the peaks:

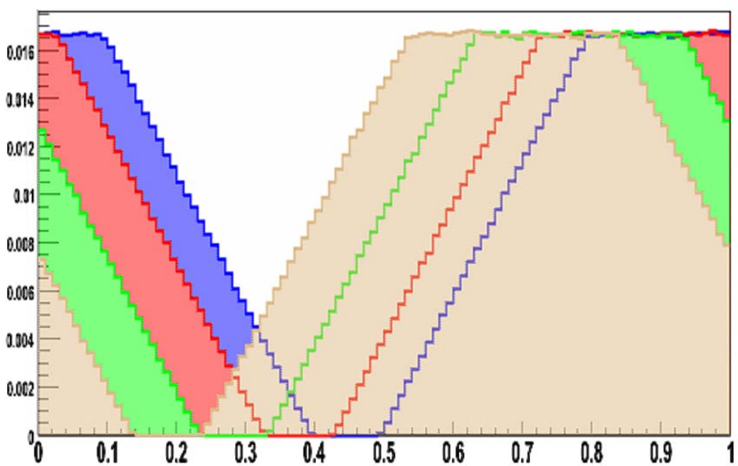

v_{beam} = 600, 400, 300, 250 m/s

8) Data analysis

- Extraction of *g*:

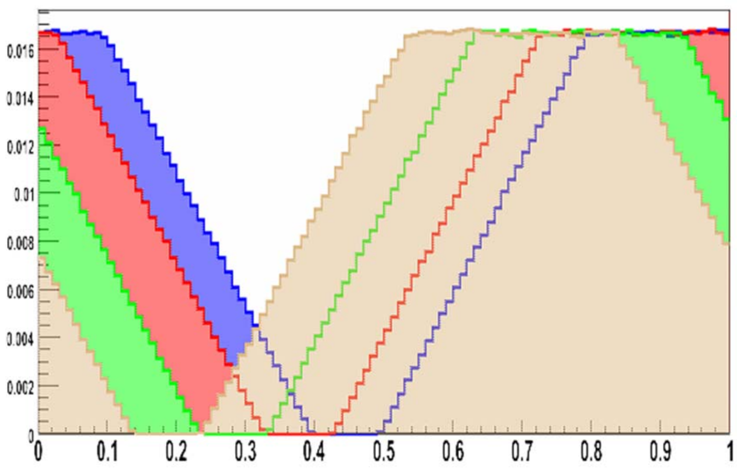

→

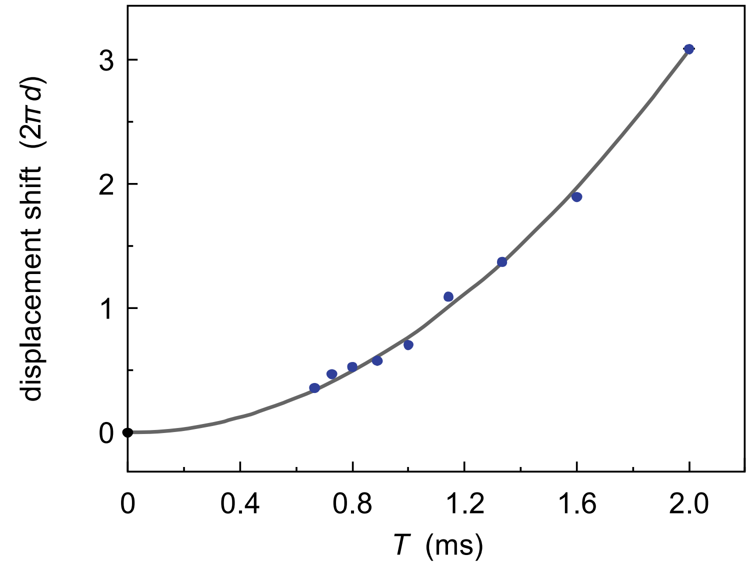

Measurement of g to 1%:

- $\approx 10^5$ $\bar{H}$ atoms at 100 mK
- 2 weeks of beam time
- Event rate: 1 Hz

$$\delta x = -gT^2 \quad = -g\,(L/v)^2$$

[M. K. Oberthaler *et al.*, Phys. Rev. A **54** (1996) 3165]

Outline

- Introduction and motivation
- AEGIS principle and setup
- Current status
- Conclusions and outlook

AEGIS construction 2010–2012

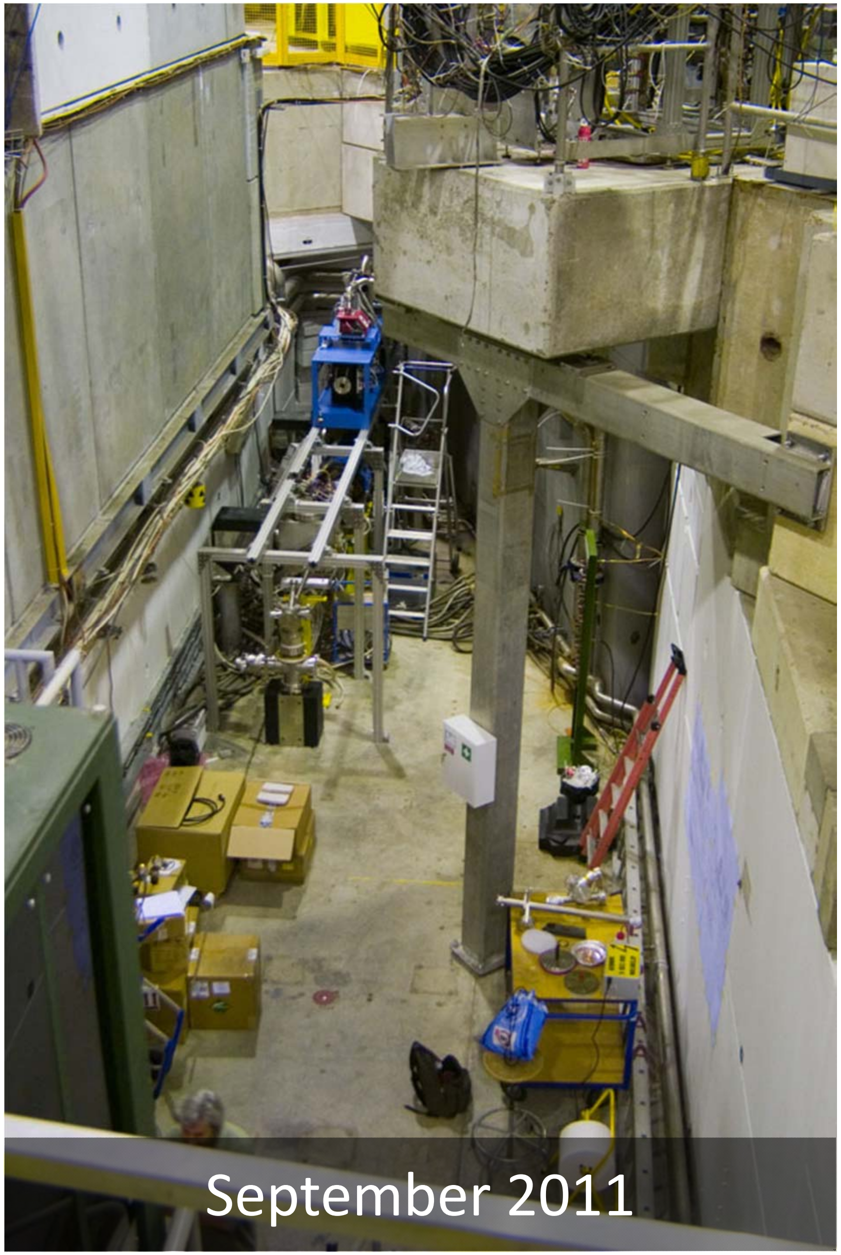

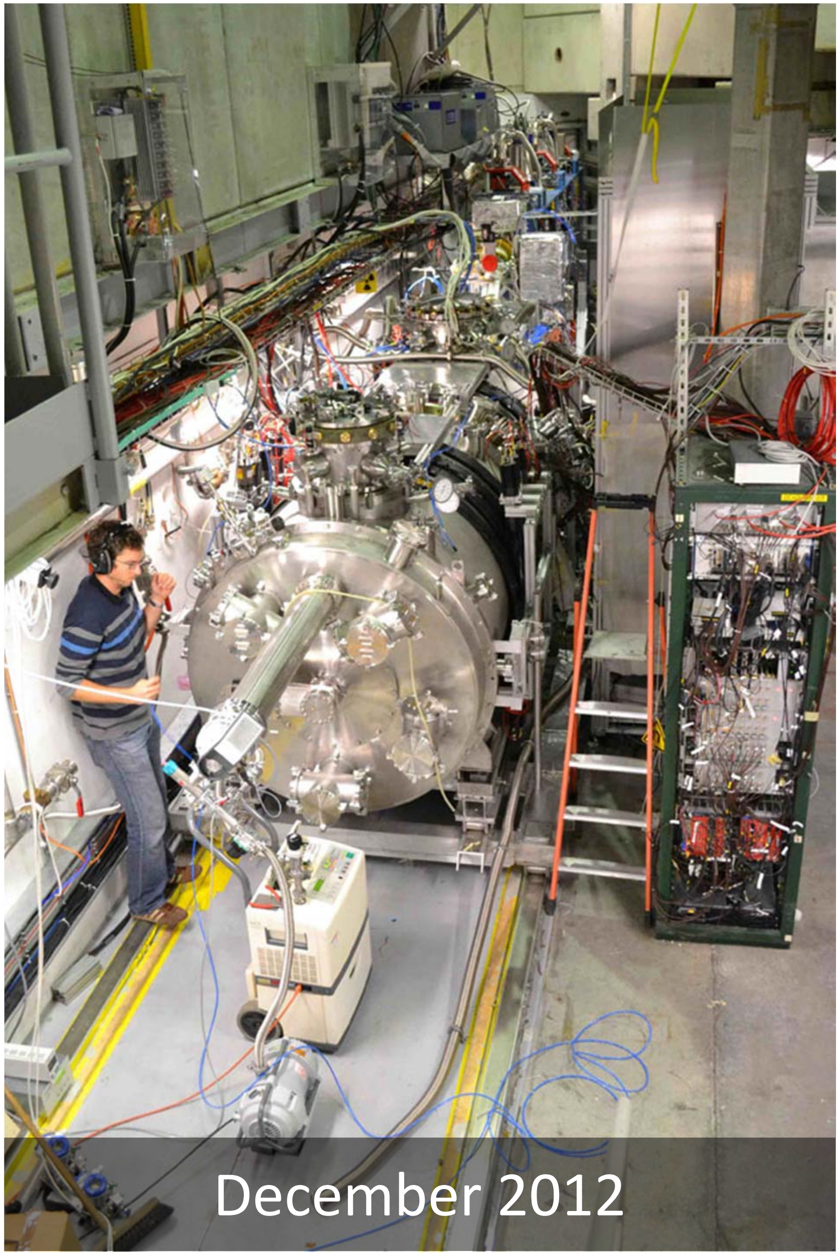

Status: Magnets and traps

- 5 T magnet (capture) and 1 T magnet ($\bar{\mathrm{H}}$ reco) installed and commissioned
- All traps completed & commissioned

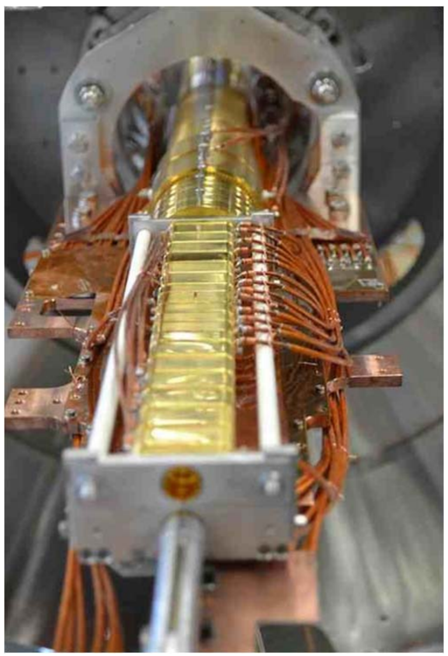

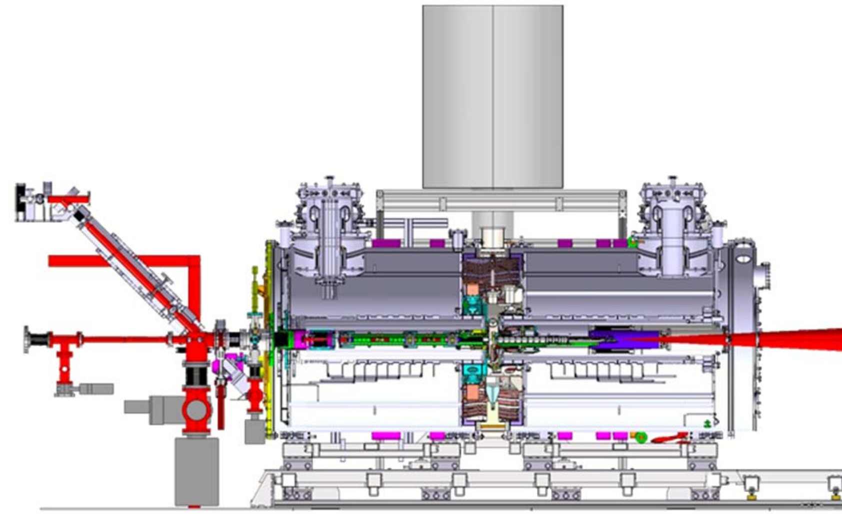

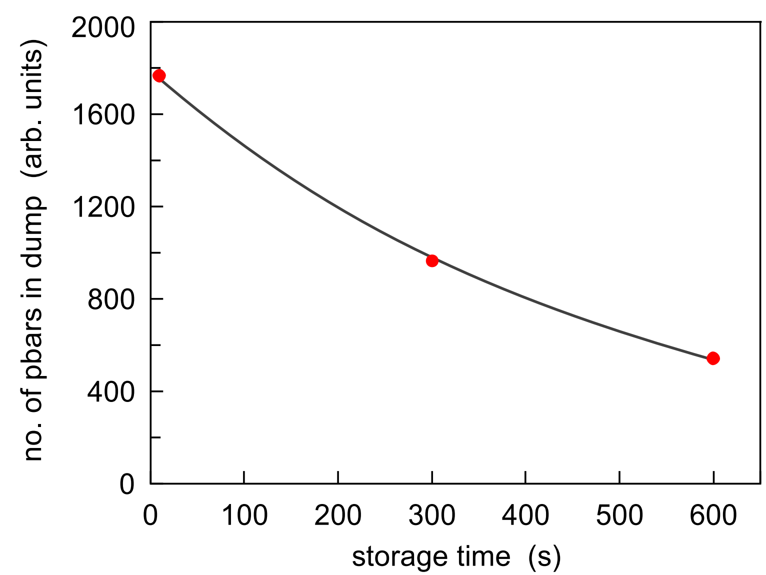

  - successful $\bar{p}$ stacking (4 shots, $4{\times}10^5$ $\bar{p}$)
  - storage of cooled $\bar{p}$ (lifetime τ = 570 s)
  - e^+ transfer to 1 T trap ($4{\times}10^5$, lifetime τ = 120 s)
  - diocotron excitation demonstrated

Status: Positronium laser

- AEGIS laser system
  for Ps excitation completed

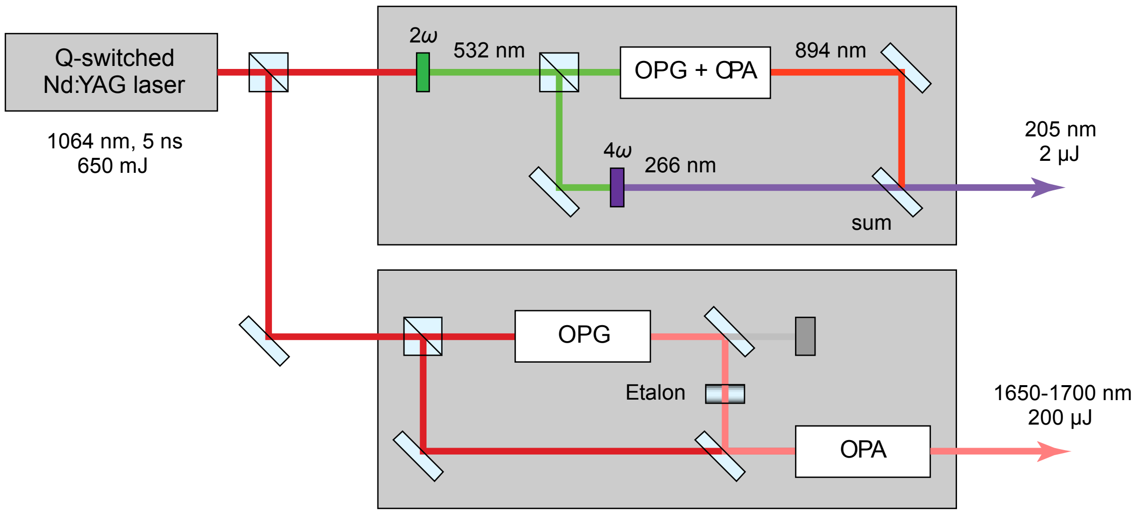

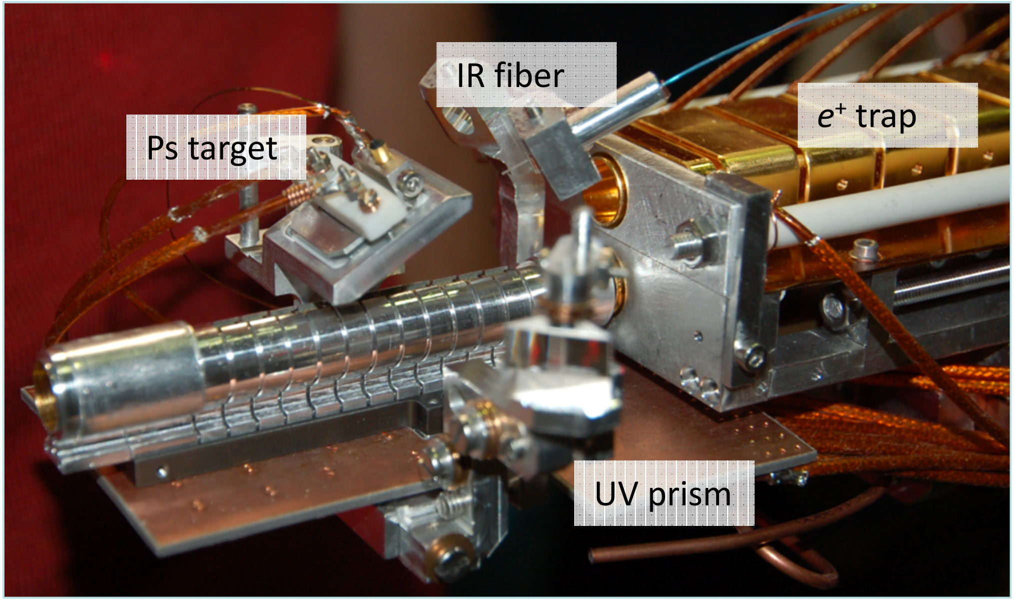

- Laser access to Ps target by
  - Prism (UV laser)
  - Fiber (IR laser)

Status: Moiré deflectometer

- Deflectometer test setup (U Heidelberg group):

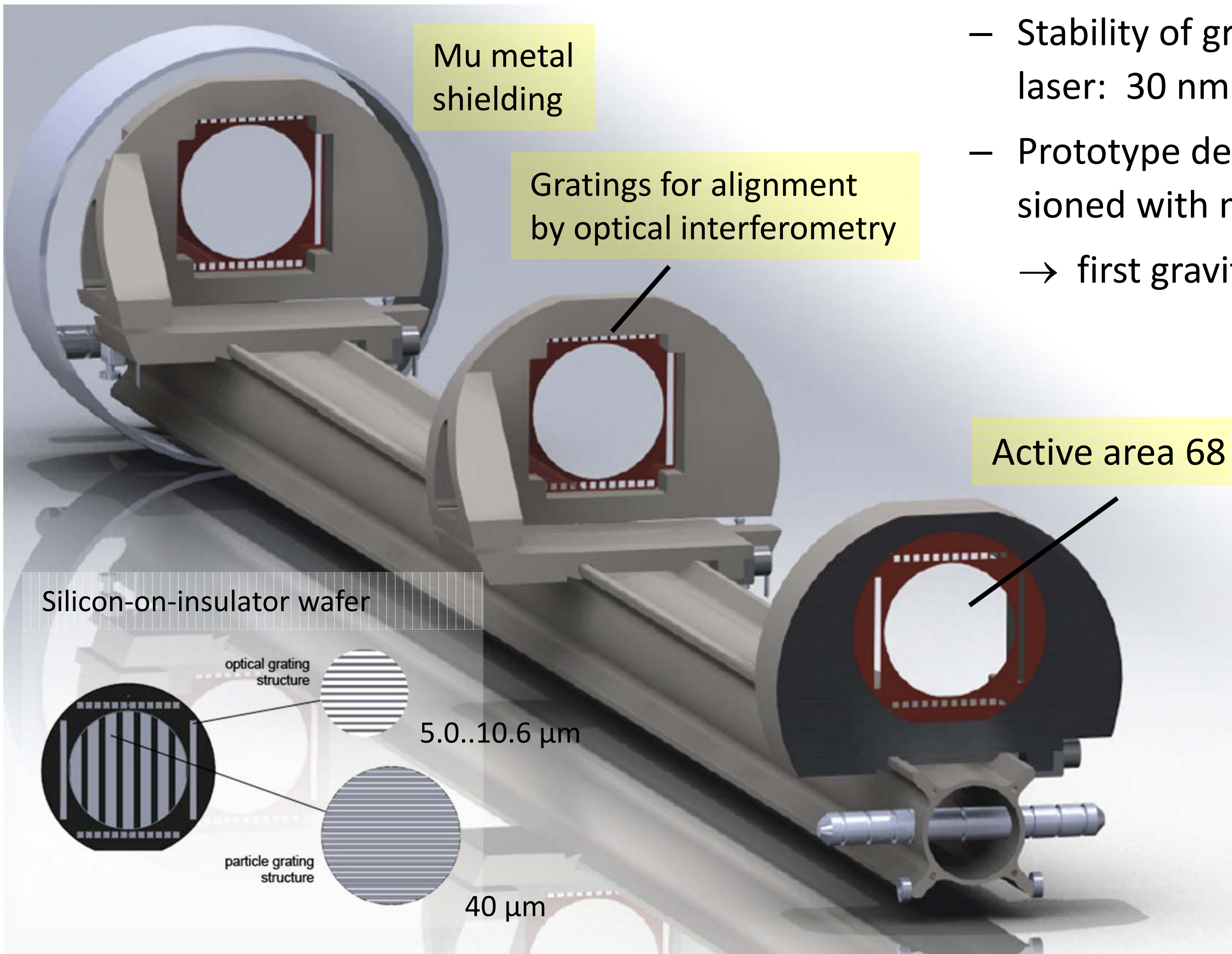

  - Stability of gratings measured with laser: 30 nm over 1 h
  - Prototype deflectometer comis-sioned with metastable Ar atoms
    $\rightarrow$ first gravity measurement

Status: Moiré $\bar{H}$ detector

- Requirement: Detect $\bar{H}$ annihilations with resolution $\Delta t \approx 1\ \mu s$, $\Delta x \approx 2\ \mu m$
- Currently favored design:

(distances and thicknesses not to scale)

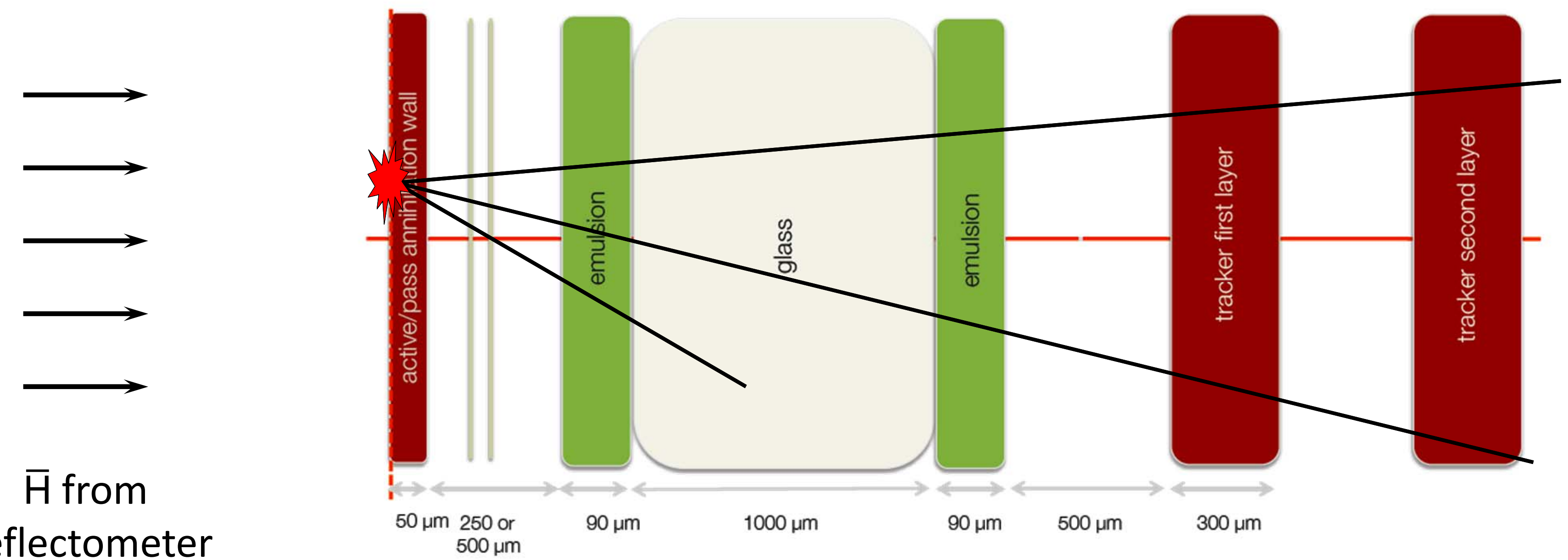

$\bar{H}$ from deflectometer

1D Si strip nuclear emulsion 2D SciFi tracker

- Time of flight from 1D Si strip
- High spatial resolution provided by emulsion
- 2D SciFi tracker correlates emulsion tracks with timed events

Status: Moiré $\overline{\mathrm{H}}$ detector

- Nuclear emulsions:
  - 90 µm thick gels on glass substrate (0.5…1 mm thick)

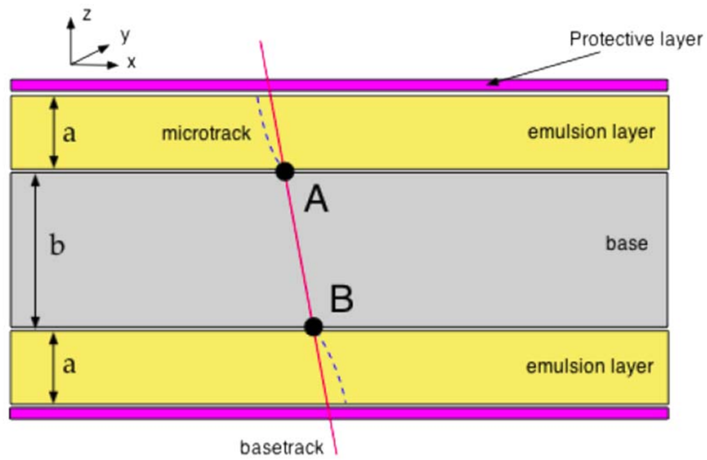

  - Based on technology developed for OPERA, modified for vacuum operation and tested at low temp
  - Off-line analysis by automatic 3D scanning microscope (3 days for 20 x 20 cm emulsion)
    $\Rightarrow$ tomographic image

Intrinsic resolution 58 nm

Vertex resolution ≈ 1.4…2.3 µm

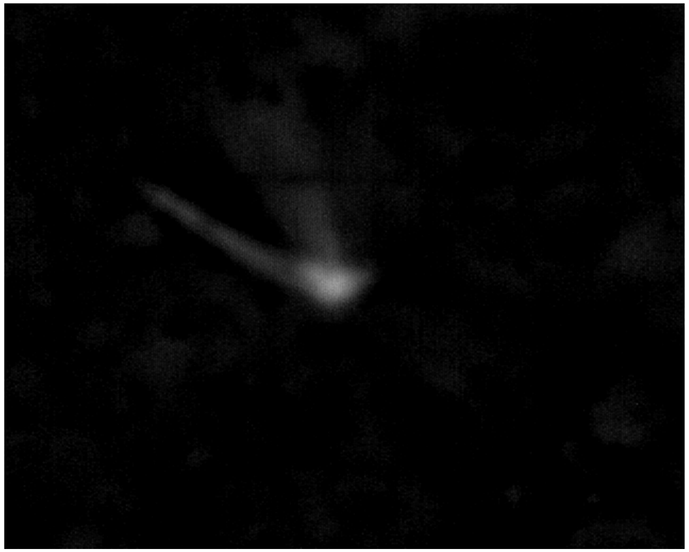

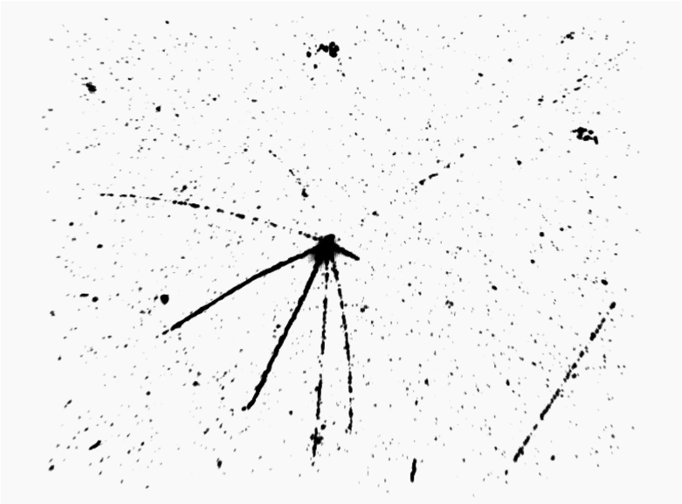

Moiré deflectometer test with $\bar{p}$

- December 2012:
  Deflectometry measurement with $\bar{p}$ in "mini moiré" setup
  - d = 40 µm, L = 25 mm
  - 110 keV $\bar{p}$, 6.5 h emulsion exposure
  - Reference measurement with diode light in Talbot-Lau regime

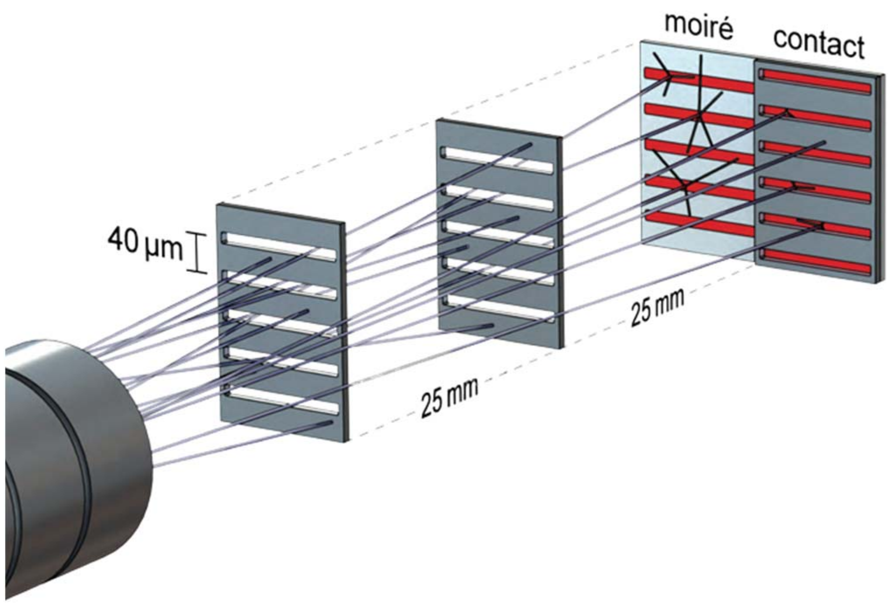

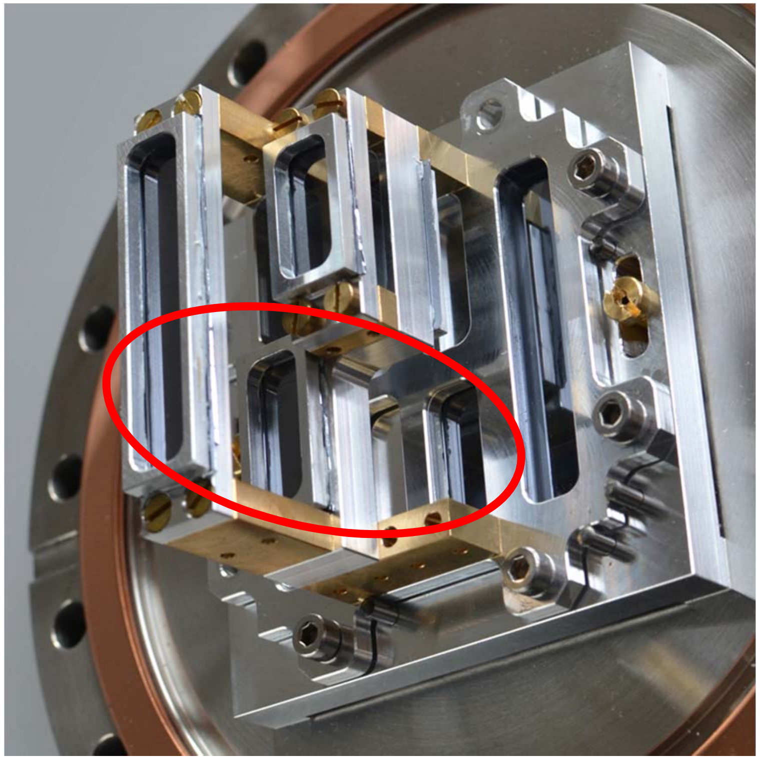

[S. Aghion *et al.*,
Nature Comm., to appear]

Moiré deflectometer test with $\bar{p}$

- Light and antiprotons detected on emulsion

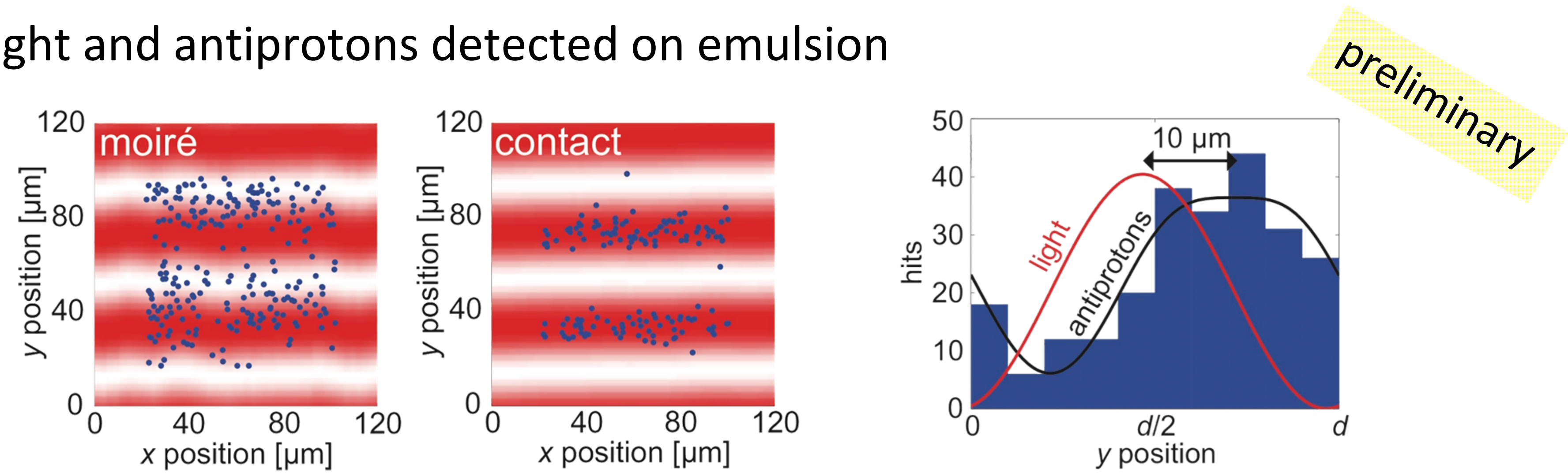

- Result:
  - Deflection (upward): 10.0 ± 0.9 (stat) ± 6.3 (syst) µm
  - Force on $\bar{p}$: 540 ± 50 (stat) ± 340 (syst) aN
  - corresponds to magnetic field ≈ 8 G or electric field ≈ 34 V/m
- Absolute shift comparable to that expected for $\bar{\mathrm{H}}$ measurement
- Force 10 orders of magnitude smaller, but sensitivity 11 orders of magnitude larger (8 for lower *v*, 3 for longer *L*)

[S. Aghion *et al.*, Nature Comm., to appear]

Outline

- Introduction and motivation
- AEGIS principle and setup
- Current status
- Conclusions and outlook

Conclusions & outlook

- The effect of gravity on antimatter has never been measured
- Depending on the chosen model, effect could be nil or dramatic
- The AEGIS experiment intends to measure g of antihydrogen to (initially) 1% precision
- Construction and commissioning of AEGIS apparatus largely completed
- Next milestones:
  - second half of 2014: $\overline{\mathrm{H}}$ formation by Ps charge exchange
  - 2015: Formation of $\overline{\mathrm{H}}$ beam
  - 2016: First antimatter gravity experiment

AEGIS Collaboration

U of Bergen / U of Oslo, Norway
A. Gligorova, N. Pacifico, O. Røhne, H. Sandaker

U of Bern / U of Zurich, Switzerland
C. Amsler, A. Ariga, T. Ariga, A. Ereditato, J. Kawada, M. Kimura, C. Pistillo, C. Regenfus, P. Scampoli, J. Storey

INFN Bologna, Italy
M. Prevedelli

CERN, Geneva, Switzerland
J. Bremer, M. Doser, A. Dudarev, S. Haider

INFN Genova, Italy
D. Krasnický, S. Di Domizio, V. Lagomarsino, G. Testera, R. Vaccarone, S. Zavatarelli

U of Heidelberg, Germany
P. Bräunig, M. K. Oberthaler

MPI-K, Heidelberg, Germany
G. Cerchiari, A. Kellerbauer, E. Jordan

University College London, UK
S. Hogan

U of Lyon, France
P. Nédélec

INFN Milano, Italy
S. Aghion, M. Caccia, R. Caravita, F. Castelli,, S. Cialdi, G. Consolati, R. Ferragut M. Giammarchi, F. Moia, F. Prelz, F. Villa

INR, Moscow, Russia
A. S. Belov, S. N. Gninenko, V. A. Matveev

Laboratoire Aimé Cotton, Orsay, France
L. Cabaret, D. Comparat

INFN Padova/Trento, Italy
R. S. Brusa, L. Di Noto, S. Mariazzi, G. Nebbia

INFN Pavia/Brescia, Italy
G. Bonomi, L. Dassa, A. Fontana, P. Genova, C. Riccardi, A. Rotondi, M. A. Subieta Vasquez

Czech Technical U, Prague, Czech Republic
V. Petráček, M. Špaček

Stefan Meyer Institute, Vienna, Austria
C. Malbrunot, E. Widmann

ETH Zurich, Switzerland
F. Merkt